CHEMISTRY
A EUROPEAN JOURNAL

DOI: 10.1002/chem.200701347

Cooperative AND Ion-Pair Recognition by Heteroditopic Calix[4]diquinone Receptors

Michael D. Lankshear,[a] Ian M. Dudley,[a] Kar-Man Chan,[a] Andrew R. Cowley,[a] Sérgio M. Santos,[b] Vitor Felix,[b] and Paul D. Beer*[a]

Abstract: A new family of heteroditopic calix[4]diquinone receptors capable of the cooperative recognition of ion-pair species through a contact binding mechanism has been developed. The receptors bind contact ion pairs cooperatively, with an unprecedented AND recognition phenomenon being observed to operate in certain cases, in which receptors display no affinity for either of the individual "free" cation or anion, but bind the cation and anion ion-pair strongly. X-ray crystallographic, solution-state, and computational methods rationalize the observed recognition behavior of the receptors. It is shown that the contact ion-pair interaction occurs through a π-stacking-mediated folding of the receptors such that the anion and cation binding sites are arranged in close proximity, while in the solid state an unusual ion-mediated receptor dimerization is observed. Molecular dynamics simulations are further used to explain the observed trends in the association constants of different ion-pair species and the mechanism of interaction.

Keywords: anions · calixarenes · cations · receptors · recognition

Introduction

The ongoing evolution of supramolecular chemistry has been, and still is, inextricably linked to the study of receptors for ionic substrates.[1] Historical developments in the field of cation recognition and sensing[2] have been recently emulated in the emergence of a large number of systems for the recognition and sensing of anions.[3] The continued interest in such receptor systems is stimulated by the multifarious roles of ions in natural and artificial systems, in both beneficial and deleterious manners. However, the designs of ion receptors studied to date are almost universally focused on the selective recognition of either a cation or an anion, which may be achieved through careful consideration of the size, geometry, and solvation properties of the target guest species. This approach, therefore, implicitly neglects the obviously important role of the counterion in controlling the strength and selectivity of the recognition process; such a shortcoming is commonly compensated for by making the counterion "non-coordinating".

An alternative paradigm for ion recognition exists, however, and involves the design of systems wherein the binding of both the cation and anion, an ion pair, can be achieved. Such an approach offers considerable benefits as the overall receptor/ion-pair complex is charge neutral and should, thus, prove advantageous in salt solubilization, extraction, detection, and membrane-transport applications.[4] Currently, this approach is reliant on two key motifs (Figure 1), wherein ion-pair recognition is achieved either through the cascade

[a] Dr. M. D. Lankshear, I. M. Dudley, K.-M. Chan, Dr. A. R. Cowley, Prof. P. D. Beer
Inorganic Chemistry Laboratory
University of Oxford, South Parks Road
Oxford, OX1 3QR (UK)
Fax: (+44) 1865-272960
E-mail: paul.beer@chem.ox.ac.uk

[b] S. M. Santos, Prof. V. Felix
Departamento de Química
CICECO, Universidade de Aveiro
3810–193, Aveiro (Portugal)

Supporting information for this article is available on the WWW under http://www.chemeurj.org/ or from the author.

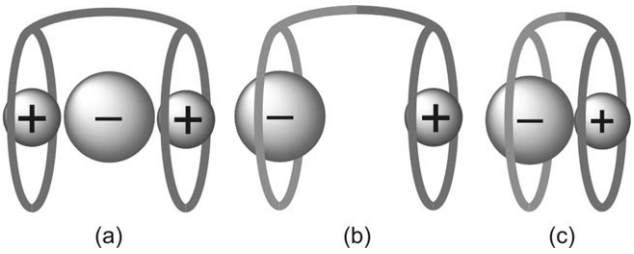

Figure 1. Different approaches for ion-pair recognition. a) Cascade, b) heteroditopic, and c) contact motifs.

approach or the use of heterotopic receptors. The former (Figure 1a) utilizes the recognition of two ions of one charge by a receptor to mediate the "trapping" of the counterion between the two recognition sites.[5] The latter (Figure 1b) relies on the incorporation of distinct anion and cation binding sites within the same molecule to achieve the recognition of multiple ions.[6] The ion-pair recognition process is ideally cooperative in nature, such that the binding of one ion enhances the binding of the other and vice versa.

The design of these heteroditopic receptors commonly relies on the separation of the two ions, which incurs an unfavorable Coulombic energy penalty. To circumvent this event, it is desirable to coordinate the ion pair such that the components are in contact (Figure 1c). Such a requirement places severe restrictions on the receptor design that can be employed, and consequently such systems are extremely rare, but recently Smith et al.[7] and Rissanen et al.[8] demonstrated the power of such an approach.

We report herein the design, synthesis, ion-binding properties, and solid-state and computational analysis of a new class of contact ion-pair receptors reliant on the proximal inclusion of calix[4]diquinone cation binding and isophthalamide-based anion binding fragments, within the same macrobicycle. In addition to supporting a contact ion-pair binding process, some of these receptors demonstrate an unprecedented binding behavior consistent with AND logic,[9] in which the receptor displays no affinity for either of the "free" cation or anion yet binds the cation and anion ion pair strongly.[10]

Results and Discussion

Receptor design and synthesis: The designs of heteroditopic receptors **1–5** (Scheme 1) have certain key features in common. They may all be generally described as polyether-based macrocycles that are capped at one end by an isophthalamide-based anion-binding fragment, which has been shown previously to bind halide anions in nonpolar organic solvents,[11,12] and anchored at the other end to a calix[4]diquinone moiety. Such calix[4]diquinone fragments have received attention previously because of their ability to bind cation species through the provision of a convergent array of electron-rich oxygen donor atoms.[13] The size of the polyether macrocycles increases in the order **1**, **2** < **3**, **4** < **5**; preliminary molecular mechanics simulations indicated that the smaller macrocycles **1** and **2** should provide an optimal spatial arrangement of the cation- and anion-binding sites for the binding of simple alkali halide ion pairs (e.g., KCl), while it was hoped that the tuning of selectivity could be achieved by increasing the macrocycle size in **3–5**. Finally, receptors **2** and **4** incorporate a nitro functionality into the anion-binding cleft of the macrocycle, which should lead to increased anion, and therefore ion pair, affinity by increasing the acidity of the amide protons.

The syntheses of these new receptors were accomplished by employing a general strategy for the formation of amide-containing macrocycle derivatives at the lower rim of the calix[4]arene and calix[4]diquinone species (Scheme 2). This strategy relies first on the selective 1,3-disubstitution of a *para-tert*-butylcalix[4]arene with a suitable asymmetric precursor (i.e., **6–8**), followed by hydrazine-mediated cleavage of the phthalimide protecting groups. The resulting bisamines **12–14** were cyclized with suitable bis(acid chloride)s in moderate to high yields to afford the macrobicycles **15–19**. Oxidation of these macrobicycles with thallium(III) trifluoroacetate[14] gave the new heteroditopic calix[4]diquinone receptors **1–5** in yields of 42–89%.

Single-crystal X-ray structures of 1 and 2: Crystals of **1** suitable for single-crystal X-ray structure determination were grown by slow diffusion of diethyl ether into a solution of the receptor in acetonitrile (Figure 2). The calix[4]arene does not adopt the cone conformation, but exists instead as a partial cone. The two *tert*-butylphenyl rings are approximately parallel, with an angle between them of 1.0°. The two quinone rings are not parallel, however, and are oriented divergently with an interplanar angle of 30.5°. Interestingly, the polyether loop of the pendant macrocycle adopts an extended conformation such that the two amide NH groups can form relatively long intramolecular hydrogen bonds to one of the oxygen atoms in the quinone unit (N···O distances: 3.171 and 3.237 Å). This intramolecular interaction suggests that the ion-binding properties of receptors **1–5** may be restricted by hydrogen-bond-mediated self-inhibition (see below).

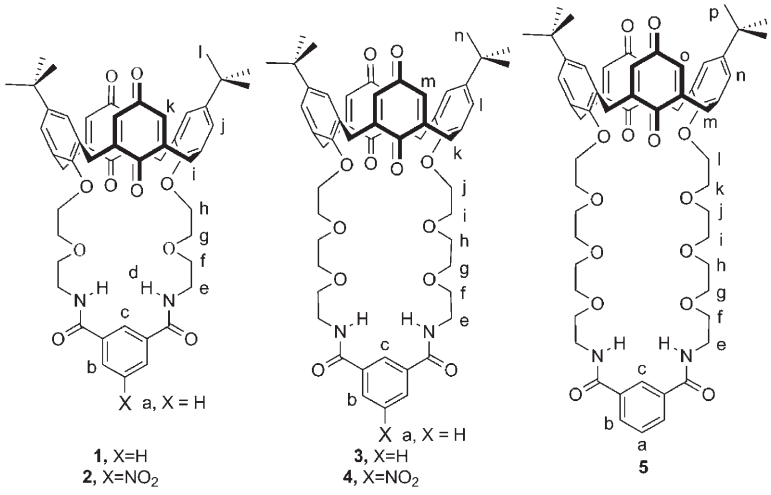

Scheme 1. Design of receptors **1–5** and proton labeling.

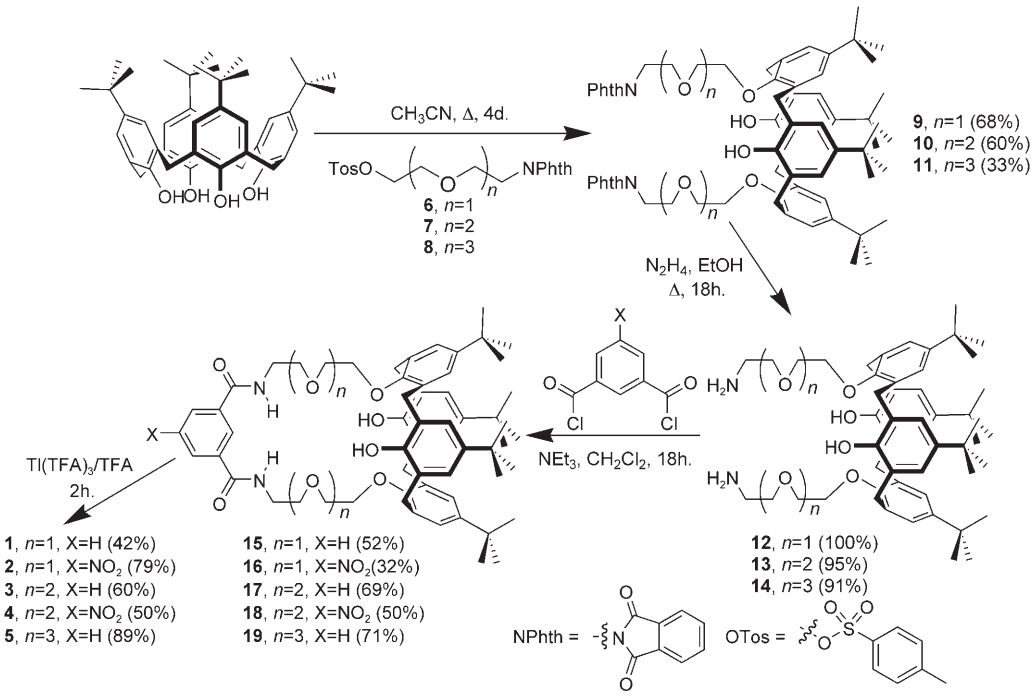

Scheme 2. Synthesis of receptors **1**–**5**.

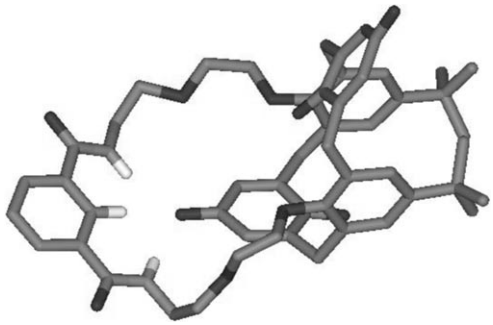

Figure 2. Single-crystal X-ray structure of **1**. Note the partial-cone conformation of the calixarene center and the presence of hydrogen-bonding interactions between the downwards facing quinone unit and isophthalamide NH units. All protons aside from those involved in hydrogen bonding have been omitted for clarity.

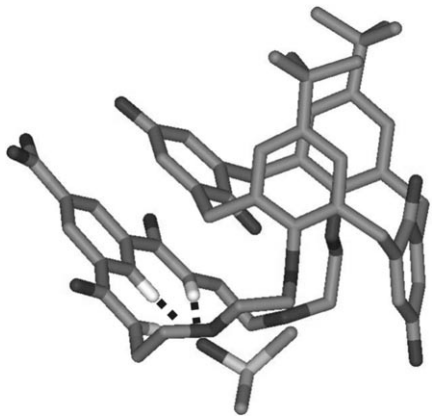

Figure 3. Single-crystal X-ray structure of **2**·DMSO. The guest DMSO molecule arises from the solvent mixture of crystallization; no DMSO was present when conducting the binding studies. Another molecule of DMSO is disordered within the structure (not shown). Hydrogen atoms not involved in hydrogen bonding have been omitted for clarity.

Single crystals of **2** were grown at the interface of a biphasic mixture of a solution of **2** in dimethyl sulfoxide (DMSO) and diisopropyl ether. The crystal structure is illustrated in Figure 3. It is notable that in the solid state **2** adopts a somewhat different structure to that of **1**. Once again the calix[4]-diquinone unit adopts a partial-cone conformation, as the two *tert*-butylphenyl rings are virtually parallel and have an interplanar angle of 2.9°, while the quinone C_6 rings are arranged divergently, with an interplanar angle of 43.9°. In this case, the nitrophenyl ring undergoes π stacking over one of these quinone rings, with a separation between the two rings of approximately 3.4 Å. Importantly, this π-stacking interaction arranges the anion and cation binding sites in proximity, which is vital to support the ion-pair recognition process. The existence of such a conformation in solution for receptors **1** and **5** (and by inference **2**) is also suggested by solution NMR spectroscopic evidence (see below). Furthermore, the oxygen atom of a guest molecule of solvent DMSO is forms hydrogen bonds with the amide group and aromatic CH donors of the receptor, with N···O separations of 3.123 and 3.07 Å, and an unusually short C···O distance of 3.04 Å.

Solution-state ion-binding properties: The study of ion-pair binding by heteroditopic receptors is complicated by the possibility of numerous solution equilibria, some of which are displayed in Scheme 3.[15] The affinity of the receptor for a single ion is defined by the processes $K_{1(\text{cation})}$ and $K_{3(\text{anion})}$,

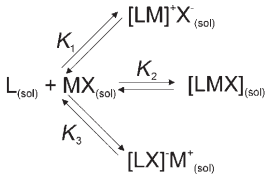

Scheme 3. Some potential solution equilibria of the interaction of a heteroditopic receptor (L) with a salt (MX). Note that further processes that correspond to the solution separation of the ion pair have been excluded for the sake of simplicity, as has the possibility of precipitation.

in which the counterion is non-coordinating, for example tetrabutylammonium (TBA) or perchlorate. The observed association constant $K_{obs(ion)}$ is generally assumed to be defined solely by these individual equilibria, in which the energetic cost of separating the anion and cation may be neglected, thus allowing the derivation of the anion and cation association constants by measuring the changes in a macroscopic observable of the receptor on addition of the analyte. Herein, such binding is assumed to represent pure cation or anion binding. The counterion is treated as completely "innocent" and therefore the anion and cation may be treated as being "free", although obviously even these non-coordinating counterions will influence ion binding to an extent. When both the cation and anion coordinate, however, these simplifications may no longer be applied, as it is no longer possible to assume that K_{obs} is representative of either K_1 or K_3, as both these processes and the extra ion-pair association equilibrium defined by K_2 are now in operation. Furthermore, the "free" ion binding properties of the receptor will be hindered in this case as the stronger ion pairing in MX renders the separation of charge implicit in the processes defined by K_1 and K_3 less likely. The commonly observed result of this is a decrease in the value of $K_{obs(ion)}$ relative to the case in which the counterion is non-coordinating; such anti-cooperative behavior occurs when the receptor design is not optimal for ion-pair binding.[16] However, when the receptor is capable of binding an ion pair, $K_{obs(ion)}$ may increase. Such a phenomenon must a result from a binding process defined by K_2, in which, for example, $K_{obs(anion)}$ may be thought of as a conflation of K_2 and K_3. This cooperative behavior indicates that the receptor is capable of binding an ion-pair species, with this capability compensating for the decrease in the single-ion affinity otherwise expected through ion pairing outside the receptor. Importantly, the direct measurement of K_2 cannot be achieved in this manner. To assess the ability of the receptors presented above to bind ion-pair species, it was therefore necessary to measure their anion and cation binding properties in the presence and absence of coordinating counterion species.

Receptors **1** and **2** were expected to provide optimal size and shape complementarity to contact ion-pair species, namely alkali metal halides. The anion-binding properties of these heteroditopic receptor systems were first assessed by ^{1}H NMR spectroscopic titration methods in [D$_3$]acetonitrile, and the addition of one equivalent of tetrabutylammonium chloride (TBACl) was found to induce only very small ($\Delta\delta = 0.01$ ppm) downfield shifts in the signals arising from the amide (d) and isophthalyl C–H (c) protons of the respective receptors. The dependence of the chemical shift on the concentration of the added chloride revealed a linear relationship, thus indicating that no anion binding was occurring; the change in chemical shift was attributed to an increase in the ionic strength of the solution. However, on the addition of one equivalent of TBACl to 1:1 mixtures of **1** or **2** and a Group 1 metal or ammonium salt, the signals arising from the amide (d) and isophthalyl (c) protons were found to broaden and shift downfield considerably ($\Delta\delta \approx 1$ ppm). This 1:1 interaction was too strong ($\log K > 4$) to allow the accurate determination of the association constant through winEQNMR[17] analysis of the titration binding curves. The same was found to be the case for sodium, potassium, and ammonium cationic guest species, although importantly no chloride ion recognition was observed in the presence of one equivalent of a non-coordinating cationic species, such as TBA or tetramethylammonium. The results illustrate a "switching on" of chloride recognition in both receptors, which appear to display absolutely no affinity for chloride in the absence of a suitable cationic guest, but which bind the halide anion very strongly when this coordinating cationic species is present.

The cation-binding properties of these systems were also probed by UV/Vis spectroscopic analysis of the respective n–π* absorption of quinone in solution with acetonitrile. With the exception of **1** and potassium, no response to the metal salts of non-coordinating anions was observed. However, when the cation salts were added to a 1:1 solution of the receptor and TBACl, significant perturbations were seen (Figure 4). SPECFIT[18] analysis of the spectra obtained allowed the calculation of 1:1 association constant values (Table 1). The cooperativity effect for **1** is most noteworthy for the binding of ammonium and sodium ions, as in these cases cation binding can only be detected in the presence of the chloride anion. No significant changes in the absorption spectra of **1** were induced on the addition of TBACl. Thus, the chloride ion can be said to "switch on" the recognition of sodium and ammonium cations through the quinone groups of **1**. Furthermore, it seems that **1** will, in some cases (e.g., for NH_4Cl and NaCl), bind the ion pair very strongly where no affinity for either of the discrete ions is observed (Scheme 3). This behavior is to our knowledge unprecedent-

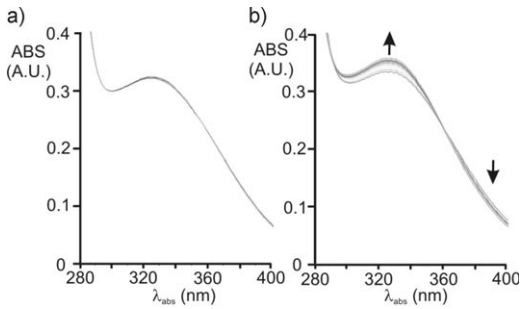

Figure 4. Enhancement of the n–π* absorbance in response to the ammonium cation. a) Absorbance response of **1** to ten equivalents of NH_4PF_6 and b) absorbance response of **1**·TBACl to ten equivalents of NH_4PF_6. Solvent: CH_3CN, temperature: 298 K, $[\mathbf{1}]_i = 0.0001$ mol dm^{-3}.

Table 1. Enhancement of cation recognition by cobound chloride ions in **1** and **2** ($\log K_{11}$).[a]

	Na^+[b]	K^+[c]	NH_4^+[c]
1	_[d]	_[d]	_[d]
1·TBACl	3.13	4.13	4.65
2	_[d]	_[d]	_[d]
2·TBACl	4.34	4.57	5.06

[a] Measurements carried out at 298 K in dry CH_3CN, spectra analyzed using the SPECFIT computer program. Errors < 15%. In the case of lithium, SPECFIT analysis of the titration data failed to give an association constant. [b] Perchlorate salt. [c] Hexafluorophosphate salt. [d] Insufficient changes in the absorption spectrum to infer cation binding.

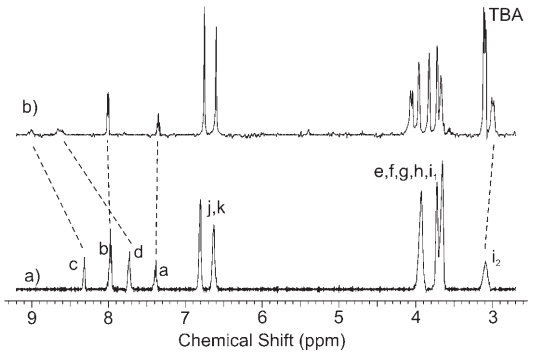

Figure 5. ^1H NMR spectra of a) **1**·NH_4PF_6 and b) **1**·NH_4Cl in D_2O/CD_3CN (2:98) at 298 K. See Scheme 1 for proton assignments.

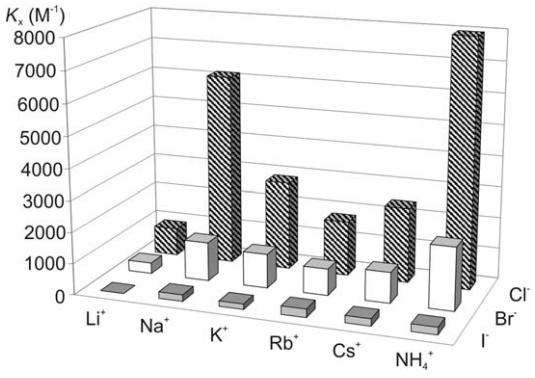

Figure 6. Anion-binding behavior of **1**·M^+ in D_2O/CD_3CN (2:98) at 298 K. WinEQNMR association constants of 1:1 were derived from monitoring proton c; error: < 10%. See the Supporting Information for a full tabulation of the chemical shifts and binding constants.

ed and can be treated through Boolean logic to show that this receptor behaves in a manner consistent with an AND gate. This finding may be rationalized thus: in the absence of a guest, **1** may be said to be in the OFF state and remains in this state (there is no perturbation of the NMR or UV/Vis spectral behavior) on the addition of the salts of "free" anions or cations with non-coordinating counterions. However, when both the cation and anion are coordinating, a strong spectral response is observed. Such behavior is consistent with the receptor functioning as an AND logic gate in which the inputs are coordinating ions.[19] A possible reason for this phenomenon could be the self-inhibition of the cation- and anion-binding sites of the molecule by intramolecular hydrogen bonding of the quinone unit with the isophthalamide motif (illustrated in the solid-state structure of **1**; Figure 2), which is disrupted only by interaction with a suitable ion pair. The enthalpic gain associated with the binding of either the anion or cation alone is not sufficient recompense to disrupt this intramolecular hydrogen-bonding interaction. Similarly for **2**, "switching on" of the cation recognition properties of the receptor occurs when the chloride anion is present. It is also interesting to note that the cation binding properties of **2**·TBACl are stronger than those of **1**·TBACl (Table 1). This behavior is most likely because of the increased acidity of the amide groups of **2**, which enhance chloride recognition, therefore leading to an improvement in the association of the MCl ion pair.

The ion-pair binding of both receptors in [D_3]acetonitrile detailed above was too strong to allow quantitative analysis of the ^1H NMR spectroscopic titration binding isotherms obtained. Changing to the more competitive solvent system 98:2 [D_3]acetonitrile/D_2O decreased the strength of the host–guest interaction, thus allowing the calculation of association constants. Peak broadening was also decreased significantly. Unsurprisingly, **1** demonstrated no affinity for TBA salts in this solvent system, as minute changes in the chemical shift arising from the amide proton (d) were observed. However, in the presence of one equivalent of a range of coordinating cations, significant downfield shifts were observed on anion addition (Figure 5), and the association constants for the 1:1 interaction could be calculated through winEQNMR analysis (Figure 6).[17]

A number of trends may be observed in these data. First, the cooperative binding of simple metal halide salts is achieved by **1** in this more competitive solvent mixture. Second, this enhancement occurs for all of the coordinating cations studied, with the halide affinity of **1** remaining chloride > bromide > iodide in all cases, as was expected on electrostatic and size–fit grounds. For iodide-containing ion pairs, only small alterations in the anion-binding properties are induced by varying the nature of the coordinated metal cation. For the anion binding of the chloride and bromide ions, however, important cation-dependent trends can be discerned. The strength of the anion association is dependent on the nature of the cation in the order $TBA^+ \ll Li^+ < Rb^+ < Cs^+ < K^+ < Na^+ < NH_4^+$. Lithium induces the smallest enhancements in anion binding, which is probably as a result of a combination of the strong solvation of "free" Li^+ and a strong LiX ion-pairing competing interaction that leads to ion-pair association outside of the receptor. There is less order to the remainder of the series; such trends arise presumably as a result of the interplay of three factors: the strength of the ion pairing of MX, hydration energies, and the size–fit relationship between the contact ion-pair MX and **1**. Thus, rubidium and cesium ions lead to weaker anion binding than potassium and sodium ions, as the latter match the size of the receptor more closely and the enthalpic gain on contact ion pairing is maximized. Through this argument, cesium chlo-

ride and cesium bromide should be bound more weakly than the rubidium analogues, but this is not the case. This behavior may be as a result of the weaker ion pairing in CsX, thus providing a less effective competing pathway to binding, or as a result of the weaker solvation of the "free" Cs^+ ion, thus allowing this large cation to bind more readily. Finally, ammonium halides are the most strongly bound, which is because of extra hydrogen-bonding interactions in the contact ion-paired species **1**·NH_4X between the bound ammonium cation and the halide anion.

Analogous ^{1}H NMR spectroscopic titration experiments with **2** produced similar results. The 1:1 association constant data derived from the winEQNMR analysis (Table 2)[17]

Table 2. Change in chemical shift induced in the 5-nitroisophthalyl H^2 proton (c) on addition of one equivalent of anion to **2** and **2**·M^+ and the relevant association constants K_{11}.[a]

	Chloride		Bromide		Iodide	
	$\Delta\delta$ [ppm]	K_{11} [M^{-1}]	$\Delta\delta$ [ppm]	K_{11} [M^{-1}]	$\Delta\delta$ [ppm]	K_{11} [M^{-1}]
2	0.03	–	0.05	–	0.01	–
2·$NaClO_4$	0.56	$>10^4$	0.33	2000	0.09	380
2·KPF_6	0.95	$>10^4$	0.53	2760	0.13	400
2·NH_4PF_6	0.90	$>10^4$	0.58	3320	0.10	320

[a] Interaction: 1:1, solvent: D_2O/CD_3CN (2:98), temperature: 298 K; association constant errors: $<10\%$.

reveal that **2** binds anions more strongly than **1** in the presence of coordinating cations, which is of course as a result of the incorporation of the electron-withdrawing nitro-functionality increasing the amide acidity. As for **1**, chloride anions are bound most strongly, followed by bromide then iodide anions, on the grounds of size and basicity. It is clear from these anion- and the above cation-association experiments (Table 1) that **2** can also behave as an AND receptor for contact ion-pair binding, for example, binding ammonium bromide where no affinity for free bromide or ammonium ions is observed. In this case, however, the behavior applies also to potassium chloride ion pairs.

The anion-binding properties of receptors **3–5** were probed in [D_6]acetone, as initial investigations using [D_3]acetonitrile-based solvent mixtures did not produce meaningful chemical-shift data. The addition of TBA salts to these receptors in [D_6]acetone induced downfield shifts in the amide (d) and isophthalyl (c) protons, thus revealing a 1:1 receptor/anion stoichiometry. The treatment of the concentration dependence of these shifts on the added anion salt yielded values of the association constants through winEQNMR analysis (Table 3).[17] These values revealed that all four receptors bound halide anions with varying strengths, although always in the expected order of $Cl^- > Br^- > I^-$.

The anion-binding constants increase in the order **3** < **5** < **4**. The observation that receptor **4** binds halides most strongly out of these systems is not particularly surprising, given that the hydrogen atoms of the amide group in this compound are rendered more acidic by the presence of the nitro

Table 3. Change in chemical shift induced in the amide proton (d) on addition of one equivalent of TBA salt to receptors **3–5** and the relevant association constants K_{11}.[a]

	3		**4**		**5**	
	$\Delta\delta$ [ppm]	K_{11} [M^{-1}]	$\Delta\delta$ [ppm]	K_{11} [M^{-1}]	$\Delta\delta$ [ppm]	K_{11} [M^{-1}]
chloride	0.42	280	0.86	1150	0.73	690
bromide	0.12	120	0.27	250	0.19	140
iodide	−0.01	–[b]	0.01	45	0.03	35

[a] Interaction: 1:1, solvent: [D_6]acetone, temperature: 298 K; association-constant error: $<10\%$. [b] No association.

group and thus are more available for hydrogen-bond donation. That **5** binds more effectively than **3** is interesting as it runs contrary to expectation based on preorganization arguments. It was postulated that the carbonyl functionality of the quinone acted as an effective hydrogen-bond acceptor unit, and thus bound to the amide hydrogen-bond donors of the isophthalamide cleft, as seen in the single-crystal X-ray structure of **1** (Figure 2). The energetic cost of folding the longer ether macrocycle in the latter receptor will decrease the likelihood of this competing intramolecular hydrogen-bond interaction, which should be weaker and therefore easier to break on ion binding.

As in the other ion-pair receptors described above, the halide affinities of **3–5** were probed by ^{1}H NMR spectroscopic methods in [D_6]acetone, in the presence of one equivalent of various coordinating cation salts. On the addition of chloride ions, the observed spectral changes were not simple to interpret. Rather than inducing a downfield shift in the protons involved in anion binding, the amide and isophthalamide signals arising from protons c and d broadened then disappeared completely after the addition of one equivalent of TBACl. New broad signals, which presumably arise from these protons, then reappeared slightly downfield after the addition of an excess of anion. This behavior could be ascribed to the equilibration between receptor and receptor·MCl being slow on the NMR timescale.[20] No chloride ion-pair association constants could therefore be obtained.

Conversely, on the addition of TBABr and TBAI salts to 1:1 mixtures of receptors **3–5** and metal cation salts, downfield shifts in the amide and isophthalyl protons d and c were observed. These shifts were larger than the corresponding changes in the chemical shift induced on the addition of the anion to the free receptors, thus suggesting an increased strength of interaction. Job-plot analysis indicated a 1:1 binding stoichiometry, and by monitoring the dependence of the chemical shift of the amide proton d as a function of the added anion concentration it was possible to obtain values for winEQNMR-derived association constants (Figure 7).[17]

It is immediately apparent from these association constants that, as for **1** and **2**, a dramatic enhancement of bromide and iodide recognition is achieved by **3–5** when a suitable coordinating cation is present. The trends in these association constants are less simple to explain, although a consideration of the cooperativity factors, which are defined by

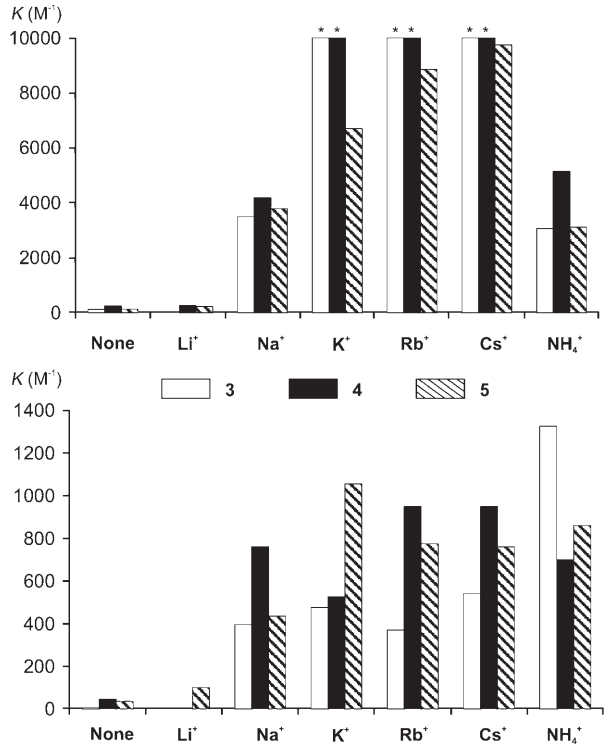

Figure 7. WinEQNMR-derived 1:1 association constants [M^{-1}] for the association of **3**–**5** with anions in the presence and absence of one equivalent of the metal salt of a non-coordinating anion. Solvent: [D_6]acetone, temperature: 298 K, error: $<10\%$. Association constants of a) bromide and b) iodide ions in the presence of various cations. In certain cases binding was too strong to be calculated accurately ($K_{11}>10^4$). See the Supporting Information for a full tabulation of the chemical shifts and binding constants.

the division of $K_{obs(anion,\ ion\ pair)}$ by $K_{obs(anion,\ free)}$, is informative (Table 4). For the bromide-containing ion pairs, **4** binds very strongly, which is explicable as a result of the increased acidity of the amide units of the anion-binding cleft. It is, however, notable that the cooperativity factors exhibited by **4** are lower than for either of the other quinone-based receptors as it has the highest anion affinity to begin with. The binding properties of **3** and **5**, which differ only in the sizes of the cavities of the polyether macrocycle, are very similar. For potassium-, rubidium-, and cesium-containing ion pairs, **3** binds more strongly, while bromide binding by **5** is dependent on the metal cation in the order ammonium $\approx$ sodium $<$ potassium $<$ rubidium $\approx$ cesium. This order is roughly size dependent, presumably as a result of a combination of a better size–fit relationship and decreased ion pairing outside of the macrocycle cavity. Recognition of iodide-containing ion pairs does not seem to follow any real trends, although it is notable that **3** binds ammonium iodide particularly strongly, which potentially arises as a result of the cavity size being readily amenable to a hydrogen-bond interaction between the two bound ions.

Table 4. Cooperativity factors for anion association.[a]

	3		**4**		**5**	
	Br^-	I^-	Br^-	I^-	Br^-	I^-
lithium	–	–[b]	1.0	0.0	1.7	2.9
sodium	29.1	79.0[b]	16.8	16.9	28.1	12.4
potassium	>83.0	95.0[b]	>40.0	11.7	49.6	30.1
rubidium	>83.0	74.0[b]	>40.0	21.1	65.6	22.1
cesium	>83.0	108.0[b]	>40.0	21.1	72.2	21.7
ammonium	25.5	265.0[b]	20.6	15.6	23.1	24.6

[a] Calculated by $K_{obs,\ ion\ pair}/K_{anion,\ free}$. [b] As the binding of iodide ions by **3** was very weak, an arbitrary value of $K_{11}=5\ M^{-1}$ was assigned for the purpose of this analysis.

The n–π^* absorbance bands of **3**–**5** observed in UV/Vis spectroscopic analysis were altered by the presence of bound cations, and the perturbations observed were large enough to allow the calculation of the association constants through the use of the SPECFIT[18] computer program. (Table 5). Unfortunately, when cation salts were added to a 1:1 mixture of these quinone receptors and TBA salts (chloride, bromide) in a variety of solvents (acetone, acetonitrile, 4:1 acetonitrile/dichloromethane) SPECFIT analysis of the resulting spectral perturbations did not yield acceptable association-constant data. Thus, for these systems this method of investigating ion-pair binding cooperativity was not possible. Unlike **1** and **2**, **3**–**5** do not demonstrate AND receptor characteristics.

Table 5. UV/Vis $\log K_{11}$ values for the interaction of **3**–**5** with various cations.[a]

	Lithium[b]	Sodium[b]	Potassium[c]	Ammonium[c]
3	–[d]	–[d]	3.84	3.60
4	–[d]	–[d]	3.56	3.40
5	–[d]	4.06	4.91	4.21

[a] Solvent: CH_3CN/CH_2Cl_2 (4:1), temperature: 298 K; spectra were analyzed using the SPECFIT computer program; error: $<15\%$. [b] Perchlorate salt. [c] Hexafluorophosphate salt. [d] Insufficient changes in the absorption spectrum to infer cation binding.

This cooperative ion-pair binding by heteroditopic calix[4]diquinone-based receptors is, therefore, a general phenomenon and tolerant of changes in the macrocycle size and/or ion-binding functionality. The strength of the ion-pair binding, coupled with the additional solid-state and solution-phase evidence detailed below, is consistent with the receptors interacting with a contact ion pair.

Single-crystal X-ray structure of 1·NH_4Cl: The existence and mechanism of the contact ion-pair binding process were probed further through comparison of the single-crystal X-ray structures of the free receptors (see above) and the structure of the ion-pair complex **1**·NH_4Cl. Orange single crystals of **1**·NH_4Cl were grown by slow evaporation of a solution of the receptor and ion pair in acetonitrile/water to give the single-crystal X-ray structure (Figure 8). This structure has a number of interesting features. The calix[4]diquinone portion of **1** is in a pinched-cone conformation, thus orienting the oxygen donor moieties of the quinone towards the bound cation, with interplanar angles of 2.7° between

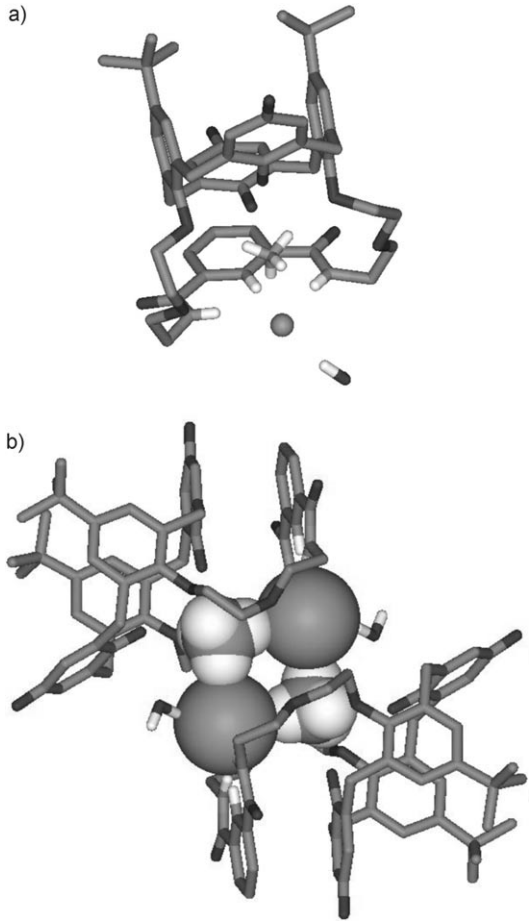

Figure 8. Single-crystal X-ray structure of **1**·NH_4Cl illustrating a) one receptor unit, NH_4Cl shown in stick representation and b) the full dimeric nature of the complex, with NH_4Cl represented as space-filling. Noninteracting hydrogen atoms have been excluded for clarity.

the phenyl rings and 53.9° between the quinone C_6 units. The cation resides in proximity to the oxygen atoms in the quinone unit with ammonium N···O distances of 2.85 and 2.68 Å, although this interaction is not supported by hydrogen bonding and is purely electrostatic in nature. However, hydrogen bonds do exist between the ammonium cation and the oxygen atoms of the macrocycle ether unit, with N···O distances of 2.98 and 3.00 Å. The chloride anion is coordinated through two amide NH···Cl and one isophthalyl CH···Cl hydrogen bonds (N···Cl: 3.29 and 3.39 Å; C···Cl: 3.49 Å), which is the expected mode of interaction within this binding cleft.[12] Furthermore, the macrocycle unit is not "planar", as initially forecast, but instead bends round to allow a π-stacking interaction between the isophthalamide aryl unit and the quinone C_6 ring. The interplanar separation is approximately 3.45 Å. This bent macrocycle allows the orientation of the cation- and anion-binding sites to allow an extremely close, or contact, ion-pair interaction between the ammonium and chloride ions (ammonium N···Cl: 3.24 Å). This close range interaction is supported by a simple hydrogen bond, with the hydrogen atom residing between the two nuclei. The chloride anion is additionally coordinated by a water molecule, with an O···Cl distance of 3.16 Å. The water molecule also forms hydrogen bonds to an oxygen atom of the quinone unit of another receptor molecule (O···O: 2.78 Å), which forces the adoption of a chain-like structure. Most remarkably, the crystal structure also demonstrates the ion-pair-mediated centrosymmetric dimerization of two molecules of receptor **1**. This dimerization occurs through two identical ammonium NH···Cl hydrogen bonds, with N···Cl distances of 3.16 Å. Coupled with the hydrogen bonding between the ion pairs bound by the individual macrocycles, this motif can be described as a "square" with the formula $(NH_4Cl)_2$, although the vertex angles are slightly off perpendicular (N-Cl-N: 84.5°; Cl-N-Cl: 95.5°). Two molecules of **1** are then arranged about this "ionic square". Such a "dimerization" of ion-paired species is not unprecedented, but is rare.[8] Each chloride anion, thus, accepts six hydrogen bonds in total, in a pseudo-octahedral manner.

Solution-state conformational analysis: The preceding solution-phase and solid-state studies raise questions about the mechanism of the contact ion-pair interaction. In particular, the crystal structure of **1**·NH_4Cl suggests that the solution-state binding phenomenon may be controlled by π stacking of the receptor to arrange the anion- and cation-binding sites in proximity, coupled with dimerization of two receptor units around an ion-pair "square". The former hypothesis was tested by ^{1}H NMR ROESY experiments conducted on **1**, **1**·NH_4Cl, and **5**. In all three cases, coupling interactions could be observed between the isophthalamide aromatic and calixquinone CH protons (see the Supporting Information). As such interactions have a distance dependence related to r^{-6}, where r is the internuclear separation, these couplings strongly suggest that the "folded" conformation of these cyclic receptors, wherein the isophthalamide unit forms π stacks above the quinone calix[4]diquinone functionality, is dominant in solution in the both "free" and ion-pair bound species. It should also be noted, however, that the single-crystal X-ray structure of **1** clearly indicates that other conformations in which hydrogen bonding rather than π stacking is the key energetic directing factor also exist. This π stacking seems to be vitally important in aiding the ion-pair recognition process by closely aligning the anion- and cation-binding motifs.

To ascertain whether or not the recognition phenomenon in solution was dimeric in nature, as suggested by the crystal structure of **1**·NH_4Cl, DOSY NMR spectroscopic experiments were carried out. The diffusion properties of two solutions of **1** and **1**·NH_4Cl in [D_3]acetonitrile were measured by using this method, which depends on the signal decay of individual peaks as a function of different pulsed-field gradient strengths. It was expected that if the species was dimeric in solution the diffusion coefficients measured by this method would vary considerably as a result of the considerable difference in the size of the two species. The diffusion constants obtained from the decay of different proton signals within the molecule (see the Supporting Information)

clearly demonstrate that there is very little difference between the diffusion properties of **1** and **1**·NH_4Cl, therefore it can be inferred that the species are of similar size. This finding strongly suggests that the receptor binds the ion pair in a monomeric fashion in solution, possibly as a result of solvation of the bound ion pair, but dimerizes on crystallization to maximize electrostatic and hydrogen-bonding interactions.

These NMR experiments, therefore, suggest that any calix[4]diquinone macrocycle containing an aromatic anion-binding cleft should be capable of supporting a contact ion-pair binding process through the proximal arrangement of anion- and cation-binding sites by π stacking. No evidence for the solution-state dimerization of the receptors was observed. A computational investigation into the process was carried out to gain further insight into the mechanism of ion-pair recognition and the trends in the observed ion-pair association.

Computational studies: Molecular modeling simulations were performed with receptors **1**, **3**, and **5** using the AMBER9[21] software package (Gaff force field).[22] The binding affinity of these three receptors towards the halide ion pairs was investigated in the gas phase and in solutions of acetonitrile or acetone by conventional molecular dynamics and free-energy calculations using the thermodynamic-integration method.

Conformational analysis in the gas phase: The lowest-energy conformations of receptor **1** and complexes **1**·KCl, **1**·NH_4Cl, **3**·KBr, and **5**·KBr were obtained through molecular-dynamics simulations at high temperature, followed by molecular-mechanics minimization. Free-receptor **1** demonstrated numerous accessible low-energy structures, consistent with a conformationally mobile species. However, in the bound ion-pair systems a striking commonality was observed between the ground-state conformations in all four cases. These confirmations were observed to be directly analogous to the single-crystal X-ray structure of **1**·NH_4Cl (Figure 8), with the ion pair bound by hydrogen bonding from the isophthalamide moiety and cation coordination by the oxygen units of the calix[4]diquinone species and polyether loop. Furthermore, even in the case of the long polyether macrocycles **3** and **5**, the isophthalamide unit forms π stacks above one of the calix[4]diquinone rings, thus allowing the close arrangement of cation- and anion-binding sites and thus the binding of contact ion-pair species. These results and the above-outlined experimental evidence suggest that this conformation is adopted on ion-pair binding, although the free receptors are conformationally mobile.

Molecular-dynamics simulations: The binding interaction of the ion pairs to receptors **1**, **3**, and **5** was investigated by molecular-dynamics simulations, wherein ion-pair MX (M = Na^+, Li^+, K^+, Rb^+, Cs^+, and NH_4^+; X = Cl^-, Br^-, and I^- for **1** and X = Br^- and I^- for **3** and **5**) was inserted into the cavity of the macrocycle of the lowest-energy conformation, as found from the conformational analyses of **1**·KCl, **1**·NH_4Cl, **3**·KBr, and **5**·KBr, and allowed to equilibrate for 150 ps. The choice of the ion-pair complexes to be simulated was governed by the available experimental data (see above). Simulations were carried out in a solution of acetonitrile for **1** and acetone for **3** and **5** over 2 ns at 300 K using a NPT (constant number of particles, pressure and temperature) ensemble and a timestep of 2 fs. During the entire time of simulation, all the cations were connected to **1**, **3**, and **5** through M···O intramolecular interactions established with two carbonyl groups and two oxygen atoms of the ether unit from the calix[4]diquinone and M···O interactions with one or two oxygen atoms of the ether species from the loops. The recognition of the halides occurred through hydrogen-bonding interactions established with two N–H binding sites of the isophthalamide cleft. The average M···O, M–X, and N–H···X distances calculated over the simulation period are given in Tables 6–11, which were measured as illustrated in Figure 9 for the **1**·KCl complex.

Table 6. Average M···O distances [Å] to the carbonyl groups of the calix[4]diquinone moiety.[a]

	1			**3**			**5**		
	Cl^-	Br^-	I^-	Cl^-	Br^-	I^-	Cl^-	Br^-	I^-
Li^+	2.30(28)	2.37(38)	2.19(3)	–	2.30(21)	2.24(6)	–	2.25(9)	2.19(5)
Na^+	2.60(25)	2.50(9)	2.51(8)	–	2.53(11)	2.50(5)	–	2.51(5)	2.49(3)
K^+	2.83(13)	2.84(13)	2.83(6)	–	2.81(7)	2.83(6)	–	2.76(2)	2.76(3)
Rb^+	3.00(16)	2.98(13)	2.95(6)	–	2.96(5)	2.95(1)	–	2.88(1)	2.91(5)
Cs^+	3.18(10)	3.19(14)	3.16(6)	–	3.14(3)	3.14(4)	–	3.16(8)	3.14(1)
NH_4^+	2.92(12)	2.90(9)	2.89(6)	2.91(9)	2.93(12)	2.90(7)	2.87(2)	2.85(1)	2.85(4)

[a] Obtained from 2 ns of molecular-dynamics simulations in solution. Values in parenthesis correspond to the standard deviation of the mean, with $n = 10000$. For the definition of the distances, see Figure 9.

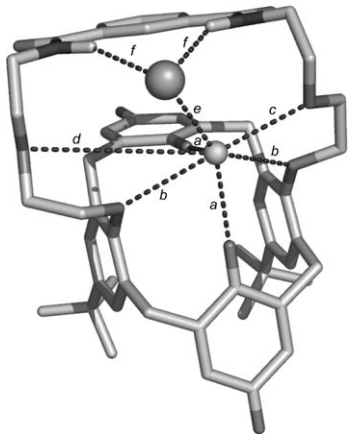

Figure 9. Molecular-mechanics structure of the **1**·KCl complex showing the measured distances: *a*) M···O(carbonyl) *b*) M···O(ether) of the calix[4]arene moiety, *c*) M···O(ether) of loop 1, *d*) M···O(ether) of loop 2, *e*) M–X, and *f*) N–H···X. CH hydrogen atoms have been excluded for clarity.

Table 7. Average M···O distances [Å] to the oxygen atoms of the calix[4]diquinone ether moieties.[a]

	1			3			5		
	Cl^-	Br^-	I^-	Cl^-	Br^-	I^-	Cl^-	Br^-	I^-
Li^+	2.81(54)	2.87(64)	2.73(37)	–	2.82(65)	2.81(3)	–	2.75(44)	2.71(25)
Na^+	2.96(22)	2.96(23)	2.96(23)	–	2.98(3)	2.96(6)	–	2.90(13)	2.89(8)
K^+	3.19(16)	3.21(25)	3.18(2)	–	3.18(15)	3.21(5)	–	3.10(3)	3.13(2)
Rb^+	3.31(25)	3.31(23)	3.30(23)	–	3.29(21)	3.32(8)	–	3.21(1)	3.23(14)
Cs^+	3.49(12)	3.50(25)	3.48(21)	–	3.46(18)	3.51(6)	–	3.45(2)	3.45(1)
NH_4^+	3.24(1)	3.23(13)	3.22(15)	3.22(1)	3.23(7)	3.23(11)	3.17(5)	3.16(1)	3.17(7)

[a] Obtained from 2 ns of molecular-dynamics simulations in solution. Values in parenthesis correspond to the standard deviation of the mean, with $n=10000$. For the definition of the distances, see Figure 9.

Table 8. Average M···O distances [Å] to the oxygen atoms of the ether unit in loop 1.[a]

	1			3			5		
	Cl^-	Br^-	I^-	Cl^-	Br^-	I^-	Cl^-	Br^-	I^-
Li^+	4.25(39)	4.12(54)	4.19(46)	–	4.88(36)	4.79(45)	–	4.26(50)	4.86(46)
Na^+	3.08(38)	3.80(58)	3.84(67)	–	3.92(55)	4.18(71)	–	3.27(55)	3.46(69)
K^+	3.18(38)	3.53(59)	3.58(61)	–	4.45(62)	3.60(73)	–	3.20(36)	3.29(37)
Rb^+	3.50(54)	3.40(48)	3.61(55)	–	3.75(66)	4.36(92)	–	3.25(36)	3.38(42)
Cs^+	3.67(33)	3.36(26)	3.43(32)	–	3.63(50)	3.44(44)	–	3.83(59)	3.52(55)
NH_4^+	3.37(69)	3.37(58)	3.42(58)	3.17(47)	3.08(36)	3.18(61)	3.12(43)	3.15(35)	3.41(83)

[a] Obtained from 2 ns of molecular-dynamics simulations in solution. Values in parenthesis correspond to the standard deviation of the mean, with $n=10000$. For the definition of the distances, see Figure 9.

Table 9. Average M···O distances [Å] to the oxygen atoms of the ether unit in loop 2.[a]

	1			3			5		
	Cl^-	Br^-	I^-	Cl^-	Br^-	I^-	Cl^-	Br^-	I^-
Li^+	4.59(26)	4.16(29)	4.47(31)	–	4.63(34)	4.66(58)	–	4.79(51)	5.38(36)
Na^+	4.61(50)	4.90(29)	4.52(33)	–	4.81(44)	4.97(48)	–	4.90(51)	5.18(51)
K^+	4.91(40)	4.49(31)	4.62(35)	–	4.84(45)	5.16(45)	–	3.86(71)	4.7(1.1)
Rb^+	4.39(44)	4.50(31)	4.59(31)	–	5.02(42)	4.34(83)	–	4.43(86)	4.7(1.1)
Cs^+	4.41(40)	4.49(31)	4.61(30)	–	5.07(43)	4.53(73)	–	3.54(54)	6.15(40)
NH_4^+	4.54(79)	4.78(47)	4.68(31)	4.86(53)	4.91(51)	5.11(45)	3.9(1.1)	3.06(38)	5.91(35)

[a] Obtained from 2 ns of molecular-dynamics simulations in solution. Values in parenthesis correspond to the standard deviation of the mean, with $n=10000$. For the definition of the distances, see Figure 9.

Table 10. Average M···X distances [Å].[a]

	1			3			5		
	Cl^-	Br^-	I^-	Cl^-	Br^-	I^-	Cl^-	Br^-	I^-
Li^+	2.18(6)	2.20(6)	2.55(9)	–	2.21(6)	2.54(9)	–	2.21(6)	2.55(9)
Na^+	2.48(7)	2.49(7)	2.78(9)	–	2.49(7)	2.77(9)	–	2.50(7)	2.79(9)
K^+	2.74(8)	2.75(8)	3.00(10)	–	2.75(8)	2.99(10)	–	2.75(8)	2.99(10)
Rb^+	2.84(9)	2.85(9)	3.10(10)	–	2.84(9)	3.08(10)	–	2.84(8)	3.08(10)
Cs^+	3.02(9)	3.02(10)	3.25(12)	–	3.00(9)	3.23(11)	–	3.00(9)	3.23(11)
NH_4^+	3.00(8)	3.04(8)	3.39(11)	3.01(8)	3.04(8)	3.40(11)	3.01(8)	3.04(8)	3.40(11)

[a] Obtained from 2 ns of molecular-dynamics simulations in solution. Values in parenthesis correspond to the standard deviation of the mean, with $n=10000$. For the definition of the distances, see Figure 9.

Table 11. Average X···H distances [Å] to the amide hydrogen atoms.[a]

	1			3			5		
	Cl^-	Br^-	I^-	Cl^-	Br^-	I^-	Cl^-	Br^-	I^-
Li^+	2.53(1)	2.55(8)	4.93(18)	–	2.53(3)	2.90(4)	–	2.63(13)	2.99(1)
Na^+	2.50(21)	2.55(4)	2.92(5)	–	2.49(1)	2.91(7)	–	2.58(7)	2.95(4)
K^+	2.49(11)	2.54(11)	2.91(6)	–	2.50(4)	2.90(11)	–	2.60(1)	2.93(1)
Rb^+	2.50(8)	2.53(8)	2.90(4)	–	2.50(2)	2.87(1)	–	2.58(1)	2.92(1)
Cs^+	2.50(2)	2.52(7)	2.89(5)	–	2.49(3)	2.88(11)	–	2.54(1)	2.92(4)
NH_4^+	2.50(7)	2.53(6)	2.89(6)	2.45(7)	2.49(8)	2.85(1)	2.54(5)	2.58(1)	2.94(8)

[a] Obtained from 2 ns of MD simulations in solution. Values in parenthesis correspond to the standard deviation of the mean, with $n=10000$. For the definition of the distances, see Figure 9.

For the three macrocycles and all the alkali cation ion pairs the distances between the metal center and the oxygen donor atoms of the calix[4]diquinone unit increase when going from Li^+ to Cs^+, thus reflecting the fitting between the cavity size of this moiety and the ion size of each cation. The cation interactions with the carbonyl groups were stronger than those with the oxygen atoms of the ether species along the course of the simulations. Consequently, the average M···O(carbonyl) distances were approximately 0.4 Å shorter than the average M···O(ether) distances, thus following the general trend found in our previous molecular-dynamics simulations between alkali cations and bis(calix[4]diquinone)-related receptors.[23] An equivalent trend in the M···O intramolecular distances was observed for the ammonium complexes, which formed N–H···O hydrogen bonds during the course of the simulation. Furthermore, for both types of M···O distances (Tables 6 and 7), it is evident that these distances are almost independent of the halide ion and the dimensions of the macrocycle, which is consistent with the apparently rigid cavity of the calix[4]diquinone unit. Indeed, the most pronounced variation in the average M···O distances is found in the LiBr complexes, thus resulting in a decrease in the M···O(ether) and M···O(carbonyl) distances as the macrocyclic dimensions increase, (ca. 0.07 Å for both distances). The distances found for the M···O interactions (Tables 8 and 9), with oxygen atoms from both ether linkages, show clearly that in the three receptors the Li^+ ion is not bonded to these donor atoms, no matter the size of the ion pair. In contrast, the M···O(ether) distances between re-

ceptor **5** and the NH_4Br ion pair suggest it is likely that both oxygen atoms contribute to the cooperative binding in this case. In the remaining complexes, the interactions of the cations with the polyether linkages occur mainly through one oxygen atom. The average X···H intramolecular distance shows that the halides are bonded to the N–H binding sites of the isophthalamide moiety through N–H···X hydrogen-bonding interactions. A unique exception is reported for the **1**·LiI complex, in which the binding of the iodide ion to the cleft fragment is interrupted after the first 800 ps of the simulation. The bonding interaction between the cations and halide anions is of an electrostatic nature and is therefore independent of the receptor dimensions, as clearly shown by data in Table 10. Thus, for the alkali metals, the M···Cl, M···Br, and M···I distances in the complexes increase as the size of the cation increases.

In addition to the oxygen atoms of the receptor and the halide anion, there are a significant number of acetonitrile or acetone molecules present in the first solvent shell, which can be bonded to the complex. The coordination numbers of the cations (metal or nitrogen atom of the ammonium ion) were therefore determined by establishing limits for the bond distances of 3.4 Å to the oxygen atoms of the carbonyl groups and solvent donor atoms and 3.8 Å to the oxygen atoms in the polyether linkage.[24] Three important observations may be made from these results for receptors **1**, **3**, and **5** (see the Supporting Information): First, for Li^+-containing ion-pair complexes, the coordination number of the metal cation is low (ca. 5) when considering only donors from the receptor and halide anion. This low coordination number is because the small size of this cation prevents the concomitant coordination of the oxygen atoms of the calix[4]diquinone unit and the polyether linkages. Second, bromide-containing ion pairs (except for lithium) are more tightly bound to **5** than to the smaller receptors **1** and **3**, with coordination numbers in the range 6–7. This behavior is because the macrocycle flexibility allows the adoption of a π–π-stacked conformation, which permits cooperative ion-pair binding. Finally, 1–2 solvent molecules on average form part of the cation coordination sphere, except for complexes of **1** with NH_4Cl, NH_4I, and NH_4Br, in which the ammonium cation is not coordinated by acetonitrile.

The analyses of the intramolecular bonding distances and coordination numbers show that the binding affinity of **1**, **3**, and **5** to the ions pairs is not primarily dictated by a rigid fitting between the receptor cavity and ion-pair size. For a further understanding of the binding affinities of different ion pairs to these macrocycles, it is necessary to obtain accurate estimates of the relative binding free-energy values in solution, as described below.

Free-energy calculations: Molecular dynamics coupled to integration methods have been successfully used to estimate the relative binding affinities of single ions towards a significant number of synthetic receptors. The values found include the binding of $H_2PO_4^-$ and halide (Cl^-, Br^-, and F^-) anions to calix[4]pyrrole and octafluorocalix[4]pyrrole[25] in water and organic solvents (CH_2Cl_2 and CH_3CN) and the binding of alkali cations to bis(calix[4]diquinone) ionophores in DMSO.[23] Herein, we extend the perturbation-energy calculations to the cooperative-recognition phenomenon of ion pairs by **1**, **3**, and **5**. To the best of our knowledge, our modeling study is the first example in which this methodology is used extensively for this purpose.

The differential binding affinities of **1**, **3**, and **5** to the MX ion pairs ($M = Na^+$, Li^+, K^+, Rb^+, Cs^+, and NH_4^+; $X = Cl^-$, Br^-, and I^- for **1** and $X = Br^-$ and I^- for **3** and **5**) were obtained by means of thermodynamic integration and standard thermodynamic cycles. Receptor **1** was examined in acetonitrile and **3** and **5** in acetone. The alkali cations were mutated, thus keeping the anions unchanged in solution (ion pair in the unbound state) and in complexes (ion pair in the bound state; see the Supporting Information), following the perturbation order: $Na^+ \rightarrow Li^+$,$Na^+ \rightarrow K^+ \rightarrow Rb^+ \rightarrow Cs^+$, and $NH_4^+ \rightarrow K^+$. Equivalent mutations were performed for the anions (keeping the cation constant) in the following sequence $Cl^- \rightarrow Br^- \rightarrow I^-$ for **1** and $Br^- \rightarrow I^-$ for **3** and **5**. The choice of the ion pairs to be mutated was governed by the available experimental binding data. To check the hysteresis of the perturbation simulations, selected complexed ion pairs (i.e., **3**·LiI→LiBr, **3**·CsI→RbI→KI→NaI, **5**·LiBr→NaBr, **5**·CsBr→RbBr, and **5**·CsI→RbI) were mutated in the reverse mode.[26] Identical interaction free-energy values, within 0.3 kcal mol^{-1}, were obtained for the forward and reverse simulations. In addition, the NaCl→KCl transformation was repeated in solution and in complexes (with **1**) with a longer equilibration period of 50 ps. The differences in solvation and interaction free-energy values for this ion-pair mutation, not exceeding 0.5 kcal mol^{-1}, were negligible. These outcomes are a clear indication of the accuracy obtained in each mutation simulation. Indeed, the use of a sufficiently large collection window allows the system to span a large amount of configurations and thus be statistically representative. Furthermore, the 20-ps equilibration period used resulted in small correlation times (average 0.1 ps) which, coupled to large data collection intervals (100 ps), led to small errors associated to the free-energy values of each window.[27]

The combination of the free-energy values obtained from the individual molecular-dynamics simulations allowed the construction of thermodynamic cycles for complexed and uncomplexed ion pairs (see the Supporting Information). It was therefore also possible to estimate the relative solvation energy ($\Delta G_{solvation}$) and interaction free-energy ($\Delta G_{interaction}$) for each transformation using at least two independent values. The values of these energies obtained from both direct simulations and thermodynamic cycles are given in the Supporting Information. The agreement between these two sets of results obtained for $\Delta G_{solvation}$ and $\Delta G_{interaction}$ is excellent, with energy discrepancies not exceeding 0.7 kcal mol^{-1}. An estimate of the relative free energy of binding of the receptor to the ion pair ($\Delta\Delta G_{binding}$) could then be obtained from these results. The resulting $\Delta\Delta G_{binding}$ values of **1**, **3**, and **5** to the halide ion pairs are summarized in Figures 10 and 11.

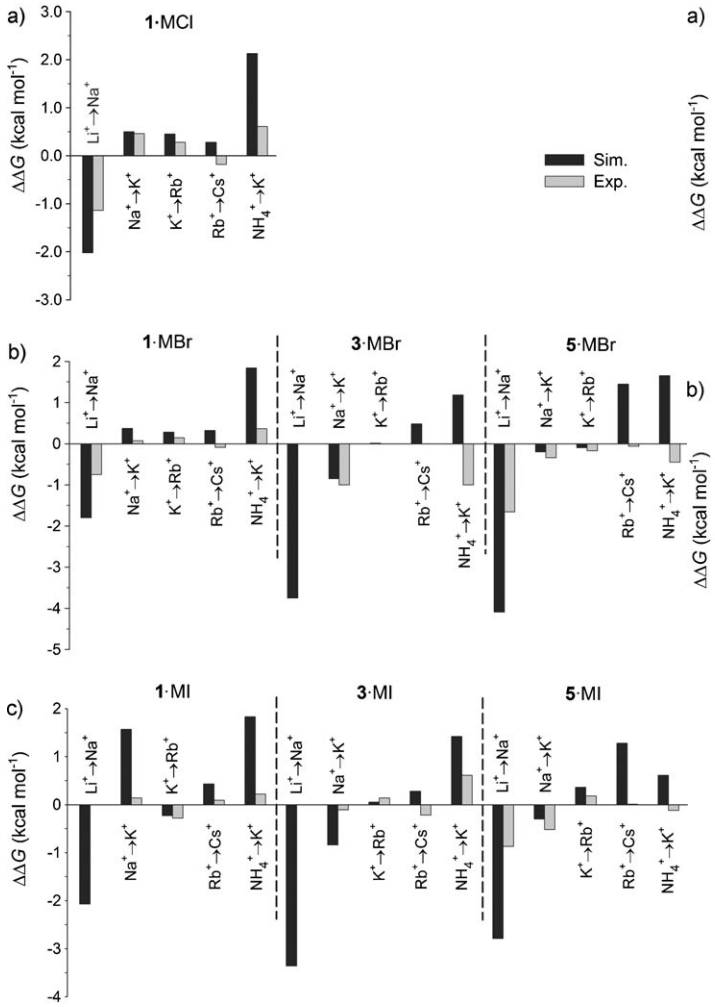

Figure 10. Relative free-energy values of binding of **1** (left column), **3** (center column), and **5** (right column) to a) MCl, b) MBr, and c) MI ion pairs (mutating cation). Values obtained directly from simulations (sim.) and the experimentally (exp.) determined binding constants. In certain cases no experimental values could be obtained. Binding constants for **1** in acetonitrile and for **3** and **5** in acetone. See the Supporting Information for the error.

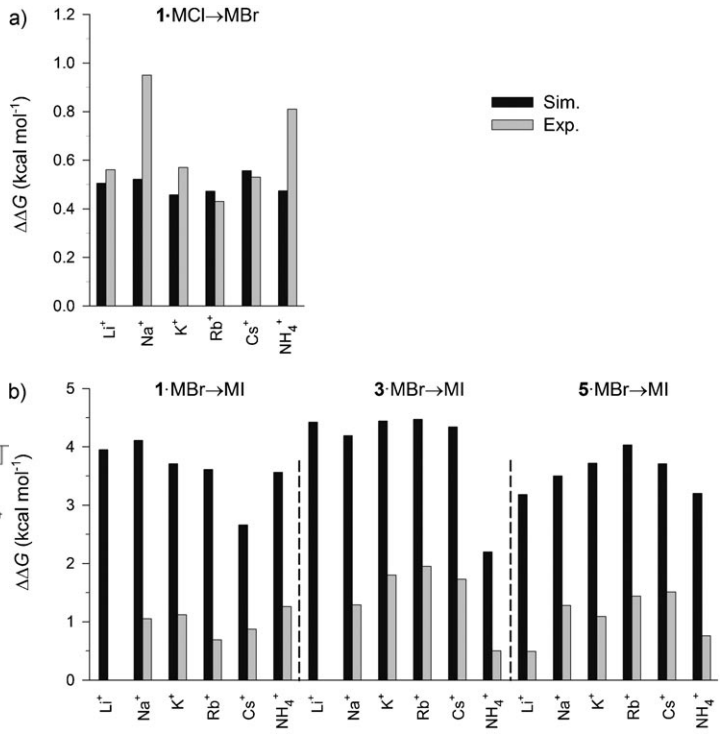

Figure 11. Relative free-energy values of binding of **1** (left column), **3** (center column), and **5** (right column) to a) MCl, b) MBr, and c) MI ion pairs (mutating anion). Values obtained directly from the simulations (sim.) and experimentally (exp.) determined binding constants. In certain cases no experimental values could be obtained. Binding constants for **1** in acetonitrile and for **3** and **5** in acetone. See the Supporting Information for the error.

Overall, there is good general agreement between the $\Delta\Delta G_{binding}$ values directly obtained from perturbation simulations and the experimental quantitative binding-constant data.[28] For example, perturbation studies in acetonitrile indicate that the selectivity for receptor **1** towards the halide ion pairs follows the order $NH_4^+ > Na^+ > K^+ > Rb^+ > Cs^+ > Li^+$, which is consistent with the experimental results for the MCl and MBr ion-pair complexes. However, the theoretical values for the $Rb^+ \rightarrow Cs^+$ mutation for the chloride and bromide ion pairs are contrary to those observed experimentally, which shows that the receptor has a binding preference for CsCl over RbCl and CsBr over RbBr. This inconsistency between the experimental and theoretical data was also found for the binding affinities of **3** to RbI and CsI and **5** to RbBr and CsBr. However, it is important to note that the experimental $\Delta\Delta G_{binding}$ values for all RbX→CsX transformations are marginal (small), and therefore such discrepancies do not allow great discussion. The calculated relative free-energy values for the **1**·RbI→CsI and **5**·RbI→CsI transformations follow the same trend as the experimental data. Concerning the $NH_4X \rightarrow KX$ mutations, the theoretical results are again largely consistent with experiment (although overestimated by ca. 1 kcal mol^{-1}) except for the bromide complexes of **3** and **5** and iodide complexes of **5**, in which the preference of the receptor for the ion pair is the opposite of that given by experiment. The theoretical calculations indicate that the NH_4X complexes are systematically more stable than the KX complexes, which was expected as the interactions between the ammonium cation and the calix[4]arene unit are moderated by electrostatic interactions and N–H···O hydrogen bonds, namely, with the oxygen atoms of the carbonyl groups, as seen from the molecular-dynamics simulations (see above), whereas interactions with the K^+ ion are only electrostatic.

It can therefore be clearly seen that apart from certain RbX→CsX and $NH_4X \rightarrow KX$ mutations the calculated and experimental $\Delta\Delta G$ values that correspond to the cationic mutation are in clear agreement (Figure 10). Other important trends may be discerned. Thus, for the LiBr→NaBr mutation, the theoretical results clearly reflect the cavity size of the receptor, since the $\Delta\Delta G$ values decrease on going from **1** to **5**. In fact, this size is further reflected in the most stable

complex of each receptor (i.e., **1**·NaBr, **3**·KBr, and **5**·RbBr), in which the receptor accommodates a larger cation as the cavity size increases.

The results obtained from anion mutation are similarly concordant with experiment. For example, the theoretical $\Delta\Delta G$ values for the **1**·MCl→MBr transformations shown in Figure 11a are in perfect agreement with the experimental values. In all mutations, the discrepancy between the values is typically within 0.4 kcal mol^{-1}, and both results indicate that the MCl complexes are more stable than the MBr complexes. Note that in the $NH_4Cl \rightarrow NH_4Br$ mutation, in which the NH_4^+ ion is kept unchanged, the calculated $\Delta\Delta G$ value is now underestimated by only 0.34 kcal mol^{-1}. This is not the case for the $NH_4Br \rightarrow NH_4I$ mutations within **1**, **3**, and **5** (Figure 11b), with the calculated $\Delta\Delta G$ values for all these mutations being systematically overestimated by approximately 3 kcal mol^{-1}. As for the other results, however, these transformations agree with experiment, since both indicate that the MBr complexes are the most stable.

These modeling results therefore show that **1** is the most appropriate receptor for the efficient recognition of small ion pairs, such as NaX and LiX (X = Cl^-, Br^-, and I^-) despite suggesting that the recognition of the latter is not thermodynamically favored relative to NaX. For larger ion pairs, such as KX (X = Br^- and I^-), receptor **3** is revealed to be the most suitable for selective recognition but is not capable of distinguishing KX from RbX. The preferential binding of the RbBr ion pair occurs with the largest receptor **5**. The efficient recognition of NH_4^+ halide ion pairs occurs almost identically by all three receptors.

Conclusion

Novel heteroditopic calix[4]diquinone receptors **1**–**5** demonstrate a new general motif for the cooperative recognition of ion pairs, with the interaction strength mediated by contact between the anion and cation. For receptors **1** and **2**, an unprecedented new phenomenon of ion-pair cooperativity termed AND recognition was discovered to operate, in which the receptor bound certain ion pairs extremely strongly (such as **1**·NH_4Cl and **2**·NaBr) where no affinity for either of the "free" ions was observed. The AND nature of the recognition is postulated to arise from the self-inhibition of the receptor by intramolecular hydrogen bonds, which may only be disrupted by the presence of both a suitable cation and anion. Although changing the ring size of the macrocycle and nature of the anion-binding site did lead to subtle differences between the binding properties of receptors **1**–**5**, the contact ion-pair interaction was not particularly discriminative between different anions. Molecular-dynamics simulations, however, provided a rationalization of the trends in the observed strength of the ion-pair binding, with the larger macrocycles preferring larger ion pairs. Further solution-phase, solid-state, and computational analyses of the receptors and the receptor/ion pair interactions provided explanation and corroboration of these results by elucidating the mechanism of ion-pair binding. This process involves the folding of the receptors to allow π-stacking interactions between the calix[4]diquinone unit and the isophthalamide fragment, thus leading to the proximal arrangement of the anion- and cation-binding sites independently of the size of the appended macrocycle. The ion pair may then bind in contact, with the differences in selectivity being determined by small differences in the rearrangement energies of the receptors. Although the solid-state evidence indicated that the process may involve dimerization of two receptors around a "square" of formula $(MX)_2$, no evidence for this arrangement could be discerned in solution. Therefore, a new class of ion-pair receptor has been elucidated. These receptors are capable of the recognition of contact ion pairs and demonstrate unprecedented AND binding behavior in certain cases.

Experimental Section

All commercial-grade chemicals were used without further purification. TBA, metal hexafluorophosphate, and perchlorate salts were stored prior to use under vacuum in a desiccator containing phosphorus pentoxide and self-indicating silica. Where quoted as dry, solvents were degassed by purging with nitrogen then dried by passing through a column of activated alumina using Grubbs apparatus. Elemental analyses were carried out by the service at the Inorganic Chemistry Laboratory, University of Oxford. Mass spectra were obtained on a Micromass LCT (ESMS) instrument. NMR spectra were recorded on a Varian Mercury 300, Oxford Instruments Venus 300, or Varian Unity Plus 500 spectrometer with the solvent serving as the lock and internal reference.

The syntheses of compounds **1**, **6**, **9**, **12**, and **15** have been described previously.[10]

2-Nitroisophthalamide diether calix[4]diquinone macrobicycle (2): This material was prepared in an analogous manner to the preparation of **1** from **16** (0.15 g, 0.15 mmol) and $[Tl(O_2CF_3)_3]$·TFA solution (4 mL). The crude product was purified by recrystallization from CH_2Cl_2/hexane to give the desired product **2** as a yellow solid (0.11 g, 79%). ^{1}H NMR (300 MHz, $CDCl_3$): δ = 1.23 (s, 18H; $C(CH_3)_3$), 3.29 (d, ^2J = 12.9 Hz, 4H; $ArH_{in}H_{out}Qu$), 3.68–3.73 (m, 12H; CH_2OCH_2 and $ArH_{in}H_{out}Qu$), 3.81 (m, 8H, $ArOCH_2$ and CH_2NH), 6.84 (s, 4H, QuH), 7.06 (s, 4H; ArH), 8.56 (br, 2H; NH), 9.05 (s, 2H; isoph ArH^4 and ArH^6), 9.12 ppm (s, 1H, isoph ArH^2); ^{13}C NMR (75.5 MHz, $CDCl_3$): δ = 197.15, 190.73, 185.48, 165.35, 154.395, 149.05, 147.47, 146.64, 135.95, 133.25, 129.27, 128.87, 126.68, 74,24, 71.59, 70.11, 41.37, 34.09, 32.58, 31.40 ppm; ESMS: *m*/*z* calcd for $C_{52}H_{59}N_4O_{12}$: 931.4136; found: 931.4129 $[M+NH_4]^+$; elemental analysis (%) calcd for $C_{52}H_{55}N_3O_{12}\cdot 2/3\,CH_2Cl_2$: C 65.2, H 5.9, N 4.3; found: C 65.3, H 5.9, N 4.1.

Isophthalamide triether calix[4]diquinone macrobicycle (3): This material was prepared in an analogous manner to the preparation of **1** from **17** (0.33 g, 0.32 mmol) and $Tl(O_2CF_3)_3$·TFA solution (5 mL). The crude product was recrystallized from diethyl ether to give the yellow receptor **3** (0.20 g, 60%). ^{1}H NMR (300 MHz, $CDCl_3$): δ = 1.07 (s, 18H; $C(CH_3)_3$), 3.25 (d, ^2J = 13.2 Hz, 4H; $ArCH_{in}H_{out}Ar$), 3.71 (m, 20H; $CH_2OCH_2CH_2OCH_2CH_2N$), 3.81 (m, 8H; $ArOCH_2$, $ArCH_{in}H_{out}Ar$), 6.77 (s, 4H; QuH), 6.86 (s, 4H; calix ArH), 7.42 (s, 2H; NH), 7.54 (t, ^3J = 7.7 Hz, 1H; isoph ArH^5), 8.07 (d, ^2J = 7.7 Hz, 2H; isoph ArH^4 and ArH^6), 8.10 ppm (s, 1H; isoph ArH^2); ^{13}C NMR (75.5 MHz, $CDCl_3$): δ = 31.41, 33.12, 34.02, 40.46, 69.69, 70.13, 70.28, 70.59, 73.22, 73.28, 123.77, 127.18, 128.98, 129.08, 131.25, 132.85, 134.40, 146.17, 147.46, 166.95, 186.59, 190.02 ppm; ESMS: *m*/*z*: 979.44 $[M+Na]^+$; elemental analysis (%) calcd for $C_{56}H_{64}N_2O_{12}\cdot 2H_2O$: C 67.7, H 6.9, N 2.8; found: C 67.5, H 6.8, N 2.7.

5-Nitroisophthalamide triether calix[4]diquinone macrobicycle (4): This material was prepared in an analogous manner to the preparation of **1** from **18** (0.15 g, 0.13 mmol) and $[Tl(O_2CF_3)_3]$·TFA solution (5 mL). The crude product was recrystallized from diethyl ether to give the yellow receptor **4** (0.08 g, 50%). ^{1}H NMR (300 MHz, $CDCl_3$): δ = 1.12 (s, 18H; $C(CH_3)_3$), 3.25 (d, ^2J = 12.9 Hz, 4H, $ArCH_{in}H_{out}Ar$), 3.71–3.85 (m, 28H; $ArOCH_2CH_2OCH_2CH_2OCH_2CH_2N$, $ArCH_{in}H_{out}Ar$), 6.80 (s, 4H; QuH), 6.85 (s, 4H; calix ArH), 7.72 (br, 2H; NH), 8.58 (s, 1H; isoph ArH^2), 8.93 ppm (s, 2H; isoph ArH^4 and H^6); ^{13}C NMR (75.5 MHz, $CDCl_3$): δ = 31.38, 32.97, 34.02, 40.65, 69.48, 70.05, 70.21, 70.62, 73.31, 125.98, 127.14, 128.89, 128.94, 132.74, 132.82, 136.38, 146.25, 147.68, 154.02, 164.56, 185.51, 190.13 ppm; ESMS: *m/z*: 1002.49 $[M+H]^+$, 1024.46 $[M+Na]^+$; elemental analysis (%) calcd for $C_{56}H_{63}N_3O_{14}\cdot 2H_2O$: C 64.8, H 6.5, N 4.0; found: C 65.0, H 6.1, N 3.9.

Isophthalamide tetraether calix[4]diquinone macrobicycle (5): This material was prepared in an analogous manner to the preparation of **1** from **19** (0.20 g, 0.17 mmol) and $[Tl(O_2CF_3)_3]$·TFA solution (5 mL). The crude product was recrystallized from diethyl ether to give the yellow receptor **5** (0.16 g, 89%). ^{1}H NMR (300 MHz, $CDCl_3$): δ = 1.05 (s, 18H; $C(CH_3)_3$), 3.18 (d, ^2J = 13.5 Hz, 4H; $ArCH_{in}H_{out}Ar$), 3.45–3.72 (m, 36H; CH_2O, CH_2N and $ArCH_{in}H_{out}Ar$), 6.60 (s, 4H; QuH), 6.78 (s, 4H; calix ArH), 7.20 (t, ^3J = 7.7 Hz, 1H; isoph ArH^5), 7.61 (s, 2H; NH), 7.99 (d, ^3J = 7.7 Hz, 2H; isoph ArH^4 and ArH^6), 8.31 ppm (s, 1H; isoph ArH^2); ^{13}C NMR (75.5 MHz, $CDCl_3$): δ = 31.37, 32.77, 34.02, 40.08, 69.69, 69.97, 70.43, 70.49, 70.64, 72.92, 125.19, 126.90, 129.04, 129.25, 130.75, 132.77, 134.62, 146.29, 147.46, 153.73, 167.03, 189.07; ESMS: *m/z*: 1067.48 $[M+Na]^+$; elemental analysis (%) calcd for $C_{60}H_{72}N_2O_{14}\cdot 1.1\,CHCl_3$: C 62.4, H 6.3, N 2.4; found: C 62.2, H 6.6, N 2.2.

5,11,17,23-Tetra-*tert*-butyl-25,27-bis{2-[2-(2-phthalimidoethoxy)ethoxy]-ethoxy}-26,28-dihydroxycalix[4]arene (10): *para-tert*-Butylcalix[4]arene (4.70 g, 7.24 mmol) and K_2CO_3 (2.10 g, 15.2 mmol) were suspended in dry CH_3CN (200 mL). Compound **7** (7.85 g, 18.1 mmol) was added, and the resulting mixture was heated to reflux for four days under a nitrogen atmosphere. After this time, the suspension was allowed to cool to room temperature, and the solvent carefully removed in vacuo to give a solid which was triturated with 1 M $HCl_{(aq)}$ (200 mL). The resulting suspension was extracted with CH_2Cl_2 (3×100 mL), after which the aqueous phase had cleared and the combined organic extracts were washed with H_2O (2×100 mL), dried over $MgSO_4$, filtered, and the filtrate concentrated in vacuo. Purification by chromatography on silica gel ($CHCl_3$/acetone = 95:5, v/v) gave the pure white solid **10** (4.97 g, 60%). ^{1}H NMR (300 MHz, $CDCl_3$): δ = 0.93 (s, 18H; $C(CH_3)_3$), 1.26 (s, 18H; $C(CH_3)_3$), 3.24 (d, ^2J = 13.2 Hz, 4H; $ArCH_{in}H_{out}Ar$), 3.72 (m, 12H; $OCH_2CH_2OCH_2CH_2O$), 3.85 (t, ^3J = 6.6 Hz, 4H; $ArOCH_2$), 3.89 (t, ^3J = 4.6 Hz, 4H; CH_2CH_2N), 4.07 (t, ^3J = 4.6 Hz, 4H; CH_2N), 4.31 (d, ^2J = 13.2 Hz, 4H; $ArCH_{in}H_{out}Ar$), 6.75 (s, 4H; calix ArH), 7.07 (s, 4H; calix ArH), 7.67 (dd, ^3J = 5.5 Hz, ^4J = 3.0 Hz, 2H; PhthH), 7.80 ppm (dd, ^3J = 5.5 Hz, ^4J = 3.0 Hz, 2H; PhthH); ESMS: *m/z*: 1193.61 $[M+Na]^+$.

5,11,17,23-Tetra-*tert*-butyl-25,27-bis(2-{2-[2-(2-phthalimidoethoxy)ethoxy]ethoxy}ethoxy)-26,28-dihydroxycalix[4]arene (11): This material was prepared in an analogous method to the preparation of **10** from *para-tert*-butylcalix[4]arene (1.36 g, 2.1 mmol), K_2CO_3 (0.70 g, 5.1 mmol), and **8** (2.52 g, 5.3 mmol) in CH_3CN (75 mL). Purification by chromatography on silica gel ($CHCl_3$/acetone = 90:10, v/v) gave the pure white solid **11** (0.79 g, 33%). ^{1}H NMR (300 MHz, $CDCl_3$): δ = 0.87 (s, 18H; $C(CH_3)_3$), 1.21 (s, 18H; $C(CH_3)_3$), 3.20 (d, ^2J = 13.1 Hz, 4H; $ArCH_{in}H_{out}Ar$), 3.60 (m, 20H; $CH_2OCH_2CH_2OCH_2CH_2O$), 3.81 (m, 8H; $ArOCH_2$, CH_2CH_2N), 4.06 (t, ^3J = 4.7 Hz, 4H; CH_2N), 4.27 (d, ^2J = 13.1 Hz, 4H; $ArCH_{in}H_{out}Ar$), 6.69 (s, 4H; calix ArH), 6.96 (s, 4H; calix ArH), 7.62 (dd, ^3J = 5.5 Hz, ^4J = 3.1 Hz, 2H; PhthH), 7.76 ppm (dd, ^3J = 5.5 Hz, ^4J = 3.1 Hz, 2H; PhthH); ESMS: *m/z*: 1281.62 $[M+Na]^+$.

5,11,17,23-Tetra-*tert*-butyl-25,27-bis{2-[2-(2-aminoethoxy)ethoxy]ethoxy}-26,28-dihydroxycalix[4]arene (13): Hydrazine monohydrate (3 mL, excess) was added to **10** (3.40 g, 2.9 mmol) was suspended in ethanol (70 mL). This suspension was then heated under reflux for 18 h, during which time the solid was seen to dissolve. The reaction mixture was allowed to cool, then added to H_2O (200 mL) to give a white suspension, which was extracted with ethyl acetate (3×50 mL). The combined organic extracts were subsequently dried over $MgSO_4$, filtered, and concentrated in vacuo to give the white solid **13** (2.51 g, 95%). ^{1}H NMR (300 MHz, $CDCl_3$): δ = 0.78 (s, 18H; $C(CH_3)_3$), 1.23 (s, 18H; $C(CH_3)_3$), 3.06 (m, 4H; CH_2NH_2), 3.24 (d, ^2J = 13.1 Hz, 4H; $ArCH_{in}H_{out}Ar$), 3.76 (m, 12H; $OCH_2CH_2OCH_2CH_2N$), 3.85 (m, 4H; $ArOCH_2CH_2$), 4.12 (m, 4H; $ArOCH_2$), 4.26 (d, ^2J = 13.1 Hz, 4H; $ArCH_{in}H_{out}Ar$), 6.58 (s, 4H; calix ArH), 7.02 ppm (s, 4H; calix ArH); ESMS: *m/z*: 911.61 $[M+H]^+$, 937.58 $[M+Na]^+$.

5,11,17,23-Tetra-*tert*-butyl-25,27-bis(2-{2-[2-(2-aminoethoxy)ethoxy]-ethoxy}ethoxy)-26,28-dihydroxycalix[4]arene (14): This material was prepared in an analogous method to the preparation of **13** from **11** (0.79 g, 0.63 mmol), ethanol (25 mL), and hydrazine monohydrate (1 mL, excess). A white solid **14** was isolated (0.52 g, 91%). ^{1}H NMR (300 MHz, $CDCl_3$): δ = 0.83 (s, 18H; $C(CH_3)_3$), 1.23 (s, 18H; $C(CH_3)_3$), 3.05 (t, ^3J = 4.4 Hz, 4H; CH_2NH_2), 3.23 (d, ^2J = 13.5 Hz, 4H; $ArCH_{in}H_{out}Ar$), 3.52 (m, 4H; CH_2CH_2N), 3.60 (m, 8H; OCH_2CH_2O), 3.68 (m, 4H; CH_2O), 3.77 (m, 4H; OCH_2), 3.88 (m, 4H; $ArOCH_2CH_2$), 4.13 (m, 4H; $ArOCH_2$), 4.26 (d, ^2J = 13.5 Hz, 4H; $ArCH_{in}H_{out}Ar$), 6.63 (s, 4H; calix ArH), 7.00 ppm (s, 4H; calixArH); ESMS: *m/z*: 999.72 $[M+H]^+$.

5-Nitroisophthalamide diether calix[4]arene macrobicycle (16): 5-Nitroisophthaloyl dichloride (1.14 mmol) was dissolved in dry CH_2Cl_2 (175 mL) and added dropwise to a stirred solution of **9** (0.98 g, 1.19 mmol) and NEt_3 (0.66 mL) in dry CH_2Cl_2 (225 mL) at 0 °C under a nitrogen atmosphere. The reaction mixture was stirred at room temperature for 3 h. The resulting solution was washed with 1 M $HCl_{(aq)}$ (2×100 mL), H_2O (2×100 mL), 1 M $NaOH_{(aq)}$ (2×100 mL), H_2O (100 mL), and brine (100 mL). The organic layer was dried over $MgSO_4$ and filtered. The filtrate was concentrated in vacuo and the residue purified by chromatography on silica gel (acetone/Et_2O = 20:80, v/v) to give a pure green solid (0.38 g, 32%). ^{1}H NMR (300 MHz, $CDCl_3$): δ = 0.95 (s, 18H; $C(CH_3)_3$), 1.15 (s, 18H; $C(CH_3)_3$), 3.25 (d, ^2J = 3.24 Hz, 4H; $ArCH_{in}H_{out}Ar$), 3.64–3.71 (m, 4H; OCH_2CH_2NH and $ArOCH_2CH_2O$), 3.77 (t, ^3J = 4.5 Hz, 4H; OCH_2CH_2N), 4.28–4.34 (m, 8H; $ArOCH_2CH_2O$ and $ArCH_{in}H_{out}Ar$), 6.95 (s, 4H; calix ArH), 6.99 (s, 4H; calix ArH), 7.47 (s, 2H; OH), 8.02 (br, 2H; NH), 8.60 (s, 2H; isoph ArH^4 and ArH^6), 8.95 ppm (s, 1H; isoph ArH^2); ESMS: *m/z* calcd for $C_{60}H_{76}N_3O_{10}$: 998.5531; found: 998.5521 $[M+H]^+$, 1020.54 $[M+Na]^+$; elemental analysis (%) calcd for $C_{60}H_{75}N_3O_{10}\cdot 0.2\,CHCl_3$: C 70.7, H 7.4, N 4.1; found: C 70.6, H 7.4, N 4.1.

Isophthalamide triether calix[4]arene macrobicycle (17): This material was prepared in an analogous manner to the preparation of **15:** Solutions of **13** (1.0 g, 1.1 mmol) in dry CH_2Cl_2 (100 mL) and isophthaloyl chloride (0.22 g, 1.1 mmol) in dry CH_2Cl_2 (100 mL) were added to a solution of triethylamine (1 mL, excess) in dry CH_2Cl_2 (800 mL). Purification by chromatography on silica gel (EtOAc/acetone = 95:5, v/v) gave the product **17** as a white solid (0.79 g, 69%). ^{1}H NMR (300 MHz, $CDCl_3$): δ = 0.89 (s, 18H; $C(CH_3)_3$), 1.30 (s, 18H; $C(CH_3)_3$), 3.25 (d, ^2J = 13.1 Hz, 4H; $ArCH_{in}H_{out}Ar$), 3.69 (m, 20H; $CH_2OCH_2CH_2OCH_2CH_2N$), 4.03 (m, 4H; $ArOCH_2$), 4.28 (d, ^2J = 13.1 Hz, 4H; $ArCH_{in}H_{out}Ar$), 6.70 (s, 4H, calix ArH), 7.05 (s, 4H; calix ArH), 7.58 (t, ^3J = 7.6 Hz, 1H; isoph ArH^5), 7.69 (br, 2H; NH), 8.11 (d, ^3J = 7.6 Hz, 2H; isoph ArH^4 and ArH^6), 8.39 ppm (s, 1H; isoph ArH^2); ESMS: *m/z* 1041.63 $[M+H]^+$, 1063.60 $[M+Na]^+$; elemental analysis (%) calcd for $C_{64}H_{84}N_2O_{10}\cdot 2H_2O$: C 71.4, H 8.2, N 2.6; found: C 71.7, H 7.9, N 2.5.

5-Nitroisophthalamide triether calix[4]arene macrobicycle (18): This material was prepared in an analogous manner to the preparation of **15**: Solutions of **13** (0.55 g, 0.60 mmol) in dry CH_2Cl_2 (75 mL) and 5-nitroisophthaloyl chloride (0.60 mmol) in dry CH_2Cl_2 (75 mL) were added to a solution of triethylamine (1 mL, excess) in dry CH_2Cl_2 (400 mL). The crude product was purified by chromatography on silica gel (EtOAc/acetone = 90:10, v/v) to give the pale-yellow solid product **18** (0.28 g, 50%). ^{1}H NMR (300 MHz, $CDCl_3$): δ = 0.84 (s, 18H; $C(CH_3)_3$), 1.31 (s, 18H; $C(CH_3)_3$), 3.21 (d, ^2J = 12.9 Hz, 4H; $ArCH_{in}H_{out}Ar$), 3.72 (m, 20H; $CH_2OCH_2CH_2OCH_2CH_2N$), 4.02 (m, 4H; $ArOCH_2$), 4.20 (m, 4H; $ArCH_{in}H_{out}Ar$), 6.62 (s, 4H; calix ArH), 7.02 (s, 4H; calix ArH), 7.78 (br, 2H; NH), 8.62 (s, 1H; isoph ArH^2), 8.79 ppm (s, 2H; ArH^4 and ArH^6); ESMS: *m/z* 1086.63 $[M+H]^+$.

Isophthalamide tetraether calix[4]arene macrobicycle (19): This material was prepared in an analogous manner to the preparation of **15**: Solutions

of **14** (0.53 g, 0.53 mmol) in dry CH_2Cl_2 (75 mL) and isophthaloyl chloride (0.11 g, 0.53 mmol) in dry CH_2Cl_2 (75 mL) were added to a solution of triethylamine (1 mL, excess) in dry CH_2Cl_2 (400 mL). Purification by chromatography on silica gel (EtOAc/acetone = 70:30, v/v) gave the product **19** as a white solid (0.43 g, 71 %). ^{1}H NMR (300 MHz, $CDCl_3$): $\delta = 0.85$ (s, 18H; $C(CH_3)_3$), 1.22 (s, 18H; $C(CH_3)_3$), 3.19 (d, $^2J = 13.1$ Hz, 4H; $ArCH_{in}H_{out}Ar$), 3.60 (m, 28H; $CH_2OCH_2CH_2OCH_2CH_2OCH_2CH_2N$), 3.92 (m, 4H; $ArOCH_2$), 4.22 (d, $^2J = 13.1$ Hz, 4H; $ArCH_{in}H_{out}Ar$), 6.67 (s, 4H; calix ArH), 6.98 (s, 4H; calix ArH), 7.48 (t, $^3J = 7.6$ Hz, 1H; isoph ArH^5), 7.78 (br, 2H; NH), 8.04 (d, $^3J = 7.6$ Hz, 2H; isoph ArH^4 and ArH^6), 8.34 ppm (s, 1H; isoph ArH^2); ESMS: m/z 1151.58 $[M+Na]^+$; elemental analysis (%) calcd for $C_{68}H_{92}N_2O_{12}\cdot 0.67\,CH_2Cl_2$: C 69.6, 7.9, N 2.4; found: C 69.6, H 8.0, N 2.2.

Acknowledgements

We thank the EPSRC and GE Healthcare for a CASE-supported studentship (to M.D.L.) and the Fundação para a Ciência e Tecnologia (FCT; to S.M.S.) for financial support (scholarship SFRH/BD/29596/2006). We further thank Drs Nick Rees and Tim Claridge (University of Oxford) for their invaluable assistance with the NMR spectroscopic studies.

[1] a) J. W Steed, J. L. Atwood, *Supramolecular Chemistry: An Introduction*, Wiley, Chichester, **2000**; b) P. D. Beer, P. A. Gale, D. K. Smith, *Supramolecular Chemistry*, OUP, Oxford, **1999**; c) J.-M. Lehn, *Supramolecular Chemistry Concepts and Perspectives*, VCH, Weinheim, **1995**.

[2] G. W. Gokel, *Molecular Recognition, Receptors for Cationic Guests, in Comprehensive Supramolecular Chemistry* (Eds.: J.-M. Lehn, J. L Atwood, J. E. D. Davies, D. D. MacNicol, F. Vogtle), *Vol. 1*, Pergamon, Oxford, **1996**.

[3] a) J. L. Sessler, P. A. Gale, W.-S. Cho, *Anion Receptor Chemistry*, RSC, Cambridge, **2006**; b) P. A. Gale, R. Quesada, *Coord. Chem. Rev.* **2006**, *250*, 3219–3244; c) K. Bowman-James, *Acc. Chem. Res.* **2005**, *38*, 671–678; d) P. A. Gale, *Coord. Chem. Rev.* **2003**, *240*, 191–221; e) P. D. Beer, P. A. Gale, *Angew. Chem.* **2001**, *113*, 502–532; *Angew. Chem. Int. Ed.* **2001**, *40*, 486–516; f) A. Bianchi, K. Bowman-James, E. García-España, *Supramolecular Chemistry of Anions*, Wiley-VCH, New York, **1997**.

[4] a) S. G. Galbraith, L. F. Lindoy, P. A. Tasker, P. G. Plieger, *Dalton Trans.* **2006**, 1134–1136; b) A. Cazacu, C. Tong, A. van der Lee, T. M. Fyles, M. Barboiu, *J. Am. Chem. Soc.* **2006**, *128*, 9541–9548; c) P. A. Tasker, V. Gasperov, in *Macrocyclic Chemistry – Current Trends and Future Perspectives* (Ed: K. Gloe), Springer, Heidelberg, **2005**, pp. 365–382; d) F. W. Kotch, V. Sidorov, Y.-F. Lam, K. J. Kayser, H. Li, M. S. Kaucher, J. T. Davis, *J. Am. Chem. Soc.* **2003**, *125*, 15140–15150; e) P. D. Beer, P. K. Hopkins, J. D. McKinney, *Chem. Commun.* **1999**, 1253–1254; f) D. J. White, N. Laing, H. Miller, S. Parsons, P. A. Tasker, S. Coles, *Chem. Commun.* **1999**, 2077–2078; g) N. Pelizzi, A. Casnati, A. Friggeri, R. Ungaro, *J. Chem. Soc. Perkin Trans. 2* **1998**, 1307–1312; h) D. M. Rudkevich, J. D. Mercer-Chalmers, W. Verboom, R. Ungaro, F. de Jong, D. N. Reinhoudt, *J. Am. Chem. Soc.* **1995**, *117*, 6124–6125; i) P. D. Beer, M. G. B. Drew, R. J. Knubley, M. I. Ogden, *J. Chem. Soc. Dalton Trans.* **1995**, 3117–3123; j) E. A. Arafa, K. I. Kinnear, J. C. Lockhart, *J. Chem. Soc. Chem. Commun.* **1992**, 61–64.

[5] a) T. Nabeshima, T. Saiki, J. Iwabuchi, S. Akine, *J. Am. Chem. Soc.* **2005**, *127*, 5507–5511; b) V. Amendola, L. Fabbrizzi, C. Mangano, P. Pallavicini, A. Poggi, A. Taglietti, *Coord. Chem. Rev.* **2001**, *219–221*, 821–837; c) L. Fabbrizzi, I. Faravelli, *Chem. Commun.* **1998**, 971–972; d) J. Cormarmond, P. Plumere, J.-M. Lehn, Y. Agnus, R. Louis, R. Weiss, O. Kahn, I. Morgenstern-Badarau, *J. Am. Chem. Soc.* **1982**, *104*, 6330–6340.

[6] a) F. Oton, A. Tarraga, A. Espinosa, M. D. Velasco, P. Molina, *Dalton Trans.* **2006**, 3685–3692; b) R. Custelcean, H. D. Laetitia, B. A. Moyer, J. L. Sessler, W.-S. Cho, S. Gross, G. W. Bates, S. J. Brooks, M. E. Light, P. A. Gale, *Angew. Chem.* **2005**, *117*, 2593–2598; *Angew. Chem. Int. Ed. Angew. Chem. Int. Ed. Engl.* **2005**, *44*, 2537–2542; c) A. Mele, P. Metrangolo, H. Neukirch, T. Pilati, G. Resnati, *J. Am. Chem. Soc.* **2005**, *127*, 14972–14973; d) J. Gong, B. C. Gibb, *Chem. Commun.* **2005**, 1393–1395; e) P. R. A. Webber, P. D. Beer, *Dalton Trans.* **2003**, 2249–2252; f) G. Tumcharern, T. Tuntulani, S. J. Coles, M. B. Hursthouse, J. D. Kilburn, *Org. Lett.* **2003**, *5*, 4971–4974; g) A. J. Evans, P. D. Beer, *Dalton Trans.* **2003**, 4451–4456; h) S. O. Kang, K. Y. Nam, *Bull. Korean Chem. Soc.* **2002**, *23*, 640–642; i) Y. H. Kim, J. I. Hong, *Chem. Commun.*, **2002**, 512–513; j) J. B. Cooper, M. G. B. Drew, P. D. Beer, *J. Chem. Soc. Dalton Trans.* **2000**, 2721–2728; k) T. Tozawa, Y. Misawa, S. Tokita, Y. Kubo, *Tetrahedron Lett.* **2000**, *41*, 5219–5223; l) S. Kubik, *J. Am. Chem. Soc.* **1999**, *121*, 5846–5855; m) S. Kubik, R. Goddard, *J. Org. Chem.* **1999**, *64*, 9475–9486; n) D. M. Rudkevich, Z. Brzozka, M. J. Palys, H. C. Viser, W. Verboom, D. N. Reinhoudt, *Angew. Chem.* **1996**, *108*, 1172–1175; *Angew. Chem. Int. Ed. Engl.* **1996**, *35*, 1090–1091; o) D. M. Rudkevich, Z. Brzozka, M. J. Palys, H. C. Visser, W. Verboom, D. N. Reinhoudt, *Angew. Chem.* **1994**, *106*, 480–482; *Angew. Chem. Int. Ed. Engl.* **1994**, *33*, 467–468; p) M. T. Reetz, C. M. Niemeyer, K. Harms, *Angew. Chem.* **1991**, *103*, 1517–1519; *Angew. Chem. Int. Ed. Engl.* **1991**, *30*, 1474–1476; q) T. Nagasaki, H. Fujishima, M. Takeuchi, S. Shinkai, *J. Chem. Soc. Perkin Trans. 1* **1995**, 1883–1888.

[7] a) J. M. Mahoney, K. A. Stucker, H. Jiang, I. Carmichael, N .R. Brinkmann, A. M. Beatty, B. C. Noll, B. D. Smith, *J. Am. Chem. Soc.* **2005**, *127*, 2922–2928; b) B. D. Smith, in *Macrocyclic Chemistry, Current Trends and Future Perspectives* (Ed.: K. Gloe), Springer, Dordrecht, **2005**, pp. 137–151; c) C. Suksai, P. Leeladee, D. Jainuknan, T. Tuntulani, N. Muangsin, O. Chailapakul, P. Kongasaeree, C. Pakavatchai, *Tetrahedron Lett.* **2005**, *46*, 2765–2769; d) J. M. Mahoney, A. M. Beatty, B. D. Smith, *Inorg. Chem.* **2004**, *43*, 5902–5907; e) J. M. Mahoney, R. A. Marshall, A. M. Beatty, B. D. Smith, S. Camiolo, P. A. Gale, *J. Supramol. Chem.* **2003**, *1*, 289–292; f) J. M. Mahoney, A. M. Beatty, B. D. Smith, *J. Am. Chem. Soc.* **2001**, *123*, 5847–5848.

[8] M. Cametti, M. Nissinen, A. Dalla Cort, L. Mandolini, K. Rissanen, *J. Am. Chem. Soc.* **2005**, *127*, 3831–3837.

[9] a) D. C. Magri, G. J. Brown, G. D. McClean, A. P. de Silva, *J. Am. Chem. Soc.* **2006**, *128*, 4950–4951; b) A. P. de Silva, H. Q. N. Gunaratne, C. P. McCoy, *J. Am. Chem. Soc.* **1997**, *119*, 7891—7892; c) A. P. de Silva, N. D. McClenaghan, Chem. Eur. J. 2004, 10, 574–586; d) A. P. de Silva, S. Uchiyama, *Nature Nanotech.* **2007**, 2, 399–410.

[10] Part of this study was published as a preliminary communication: M. D. Lankshear, A. R. Cowley, P. D. Beer, *Chem. Commun.* **2006**, 612–614.

[11] P. A. Gale, *Acc. Chem. Res.* **2006**, *39*, 465–475.

[12] a) K. Kavallieratos, C. M. Bertao, R. H. Crabtree, *J. Org. Chem.* **1999**, *64*, 1675–1683; b) K. Kavallieratos, S. R. de Gala, D. J. Austin, R. H. Crabtree, *J. Am. Chem. Soc.* **1997**, *119*, 2325–2326.

[13] a) P. Lhotak, *Top. Curr. Chem.* **2005**, *255*, 65–95; b) P .D. Beer, S. E. Matthews, *Supramol. Chem.* **2005**, *17*, 411–435; c) P. R. A. Webber, P. D. Beer, G. Z. Chen, V. Felix, M. G. B. Drew, *J. Am. Chem. Soc.* **2003**, *125*, 5774–5785; d) S. O. Kang, J. M. Oh, Y. S. Yang, J. C. Chun, S. Jeon, K. Y. Nam, *Bull. Korean Chem. Soc.* **2002**, *23*, 145–148; e) Z. Asfari, V. Bohmer, J. Harrowfield, J. Vicens, *Calixarenes 2001*, Kluwer, Dordrecht, Netherlands, **2001**; f) L. Mandolini, R. Ungaro, *Calixarenes in Action*, Imperial College Press, London, **2000**; g) P. D. Beer, P. A. Gale, Z. Chen, M. G. B. Drew, J. A. Heath, M. I. Ogden, H. R. Powell, *Inorg. Chem.* **1997**, *36*, 5880–5893; h) M. Gomez-Kaifer, P. A. Reddy, C. D. Gutsche, L. Echegoyen, *J. Am. Chem. Soc.* **1997**, *119*, 5222–5229.

[14] a) P. A. Reddy, R. P. Kashyap, W. H. Watson, C. D. Gutsche, *Isr. J. Chem.* **1992**, *32*, 89–96; b) A. McKillop, B. P. Swann, E. C. Taylor, *Tetrahedron* **1970**, *26*, 4031–4039; c) A. McKillop, J. S. Fowler, M. J. Zelesko, J. D. Hunt, E. C. Taylor, G. McGillivray, *Tetrahedron Lett.* **1969**, *10*, 2423–2426.

[15] R. Shukla, T. Kida, B. D. Smith, *Org. Lett.* **2000**, *2*, 3099–3102.

[16] H. Miyaji, S. R. Collinson, I. Prokes, J. H. R. Tucker, *Chem. Commun.* **2003**, 64–65.
[17] M. J. Hynes, *J. Chem. Soc. Dalton Trans.* **1993**, 311–312.
[18] SPECFIT, v. 2.02, Spectrum Software Associates Chapel Hill, NC, USA.
[19] A. P. de Silva, N. D. McClenaghan, *Chem. Eur. J.* **2004**, *10*, 574–586.
[20] Variable-temperature NMR spectroscopic experiments, however, indicated an independence of the phenomenon from the temperature at which the experiments were conducted, thus suggesting that slow exchange was not the correct explanation.
[21] D. A. Case, T. A. Darden, T. E. Cheatham, III, C. L. Simmerling, J. Wang, R. E. Duke, R.Luo, K. M. Merz, D. A. Pearlman, M. Crowley, R. C. Walker, W. Zhang, B. Wang, S. Hayik, A. Roitberg, G. Seabra, K. F. Wong, F. Paesani, X. Wu, S. Brozell, V. Tsui, H. Gohlke, L. Yang, C. Tan, J. Mongan, V. Hornak, G. Cui, P. Beroza, D. H. Mathews, C. Schafmeister, W. S. Ross, P. A. Kollman, AMBER9, University of California, San Francisco, **2006**.
[22] J. Wang, R. M. Wolf, J. W. Caldwell, P. A. Kollman, D. A. Case, *J. Comput. Chem.* **2004**, *25*, 1157–1174.
[23] V. Felix, M. G. B. Drew, P. R. A. Webber, P. D. Beer, *Phys. Chem. Chem. Phys.* **2006**, *8*, 521–532.
[24] The choice of these values is somewhat arbitrary since there is not a clear break down in the cation···oxygen distances, therefore these distances may be considered to be nonbonded.
[25] J. R. Blas, M. Márquez, J. L. Sessler, F. J. Luque, M. Orozco, *J. Am. Chem. Soc.* **2002**, *124*, 12796–12805.
[26] The large number of systems to be theoretically investigated, allied to the fact that a complete mutation took in 2.1 ns, would become too expensive; in terms of central processing unit (CPU) time, if all the perturbation simulations were repeated by using different starting configurations, different conditions, or if all were performed in a backward mode.
[27] a) J. L. Maccallum, D. P. Tieleman, *J. Comput. Chem.* **2003**, *24*, 1930–1935; b) G. Hummer, *J. Chem. Phys.* **2001**, *114*, 7330–7337; c) R. H. Wood, W. C. F. Mühlbauer, P. T. Thompson, *J. Phys. Chem.* **1991**, *95*, 6670–6675.
[28] Although herein we discuss only the directly obtained values, a similar discussion is possible for the majority of those values obtained from thermodynamic cycles.

Received: August 28, 2007
Revised: October 29, 2007
Published online: January 7, 2008

